Implicit Finite Volume Approximation of Nonlinear Advection-Diffusion Equations

Todd Arbogast

Center for Subsurface Modeling,
Oden Institute for Computational Engineering and Sciences
and Department of Mathematics
The University of Texas at Austin

Chieh-Sen Huang, National Sun Yat-sen Univ., Kaohsiung, Taiwan
Xikai Zhao, Mathematics, UT-Austin (now Schlumberger)
Danielle King, Mathematics, UT-Austin

This work was supported by the U.S. National Science Foundation
and the Taiwan Ministry of Science and Technology

Advection-Diffusion-Reaction Equations

$$\boxed{u_t + \nabla \cdot [f(u) - D(u)\nabla u] = g(u)}$$

Within science and engineering, researchers often use models involving

1. Advection, $u_t + \nabla \cdot f(u) = 0$
   - the transport of a substance
   - mathematically hyperbolic
2. Diffusion, $u_t - \nabla \cdot D(u)\nabla u = 0$
   - the spreading of a substance to the average of its surroundings
   - mathematically parabolic (or elliptic)
3. Reactions, $u_t = g(u)$ [Omit for this talk]
   - substances transform to other substances
   - mathematically an ordinary differential equation

These are systems of advection-diffusion-reaction equations.

Main Difficulty: The equations are often advection dominated.

> The solution to the equations can develop steep fronts or even shock discontinuities.

$$\boxed{u_t + \nabla \cdot f(u) = 0}$$

- Mass conservative
- Linear transport in 1D is simple translation

$$u_t + a u_x = 0, \;\; u(x,0) = u_0(x) \qquad \Longrightarrow \qquad u(x,t) = u_0(x - at)$$

  A discontinuity in u_0 propagates as a contact discontinuity.
- Nonlinear transport in 1D has variable speed

$$u_t + f'(u)\, u_x = 0, \;\; u(x,0) = u_0(x)$$

  If $f(u)$ grows with u, a shock discontinuity can form.

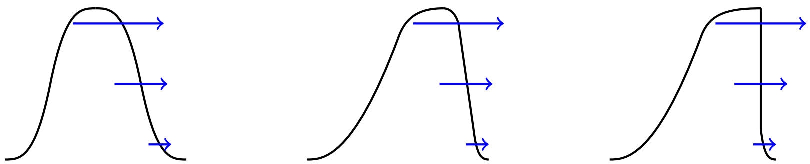

- Solutions do not become smoother in time (the operator is *not* compact), but solutions are total variation diminishing

$$\mathrm{TV}(u)(t) = \int |u_x(x,t)|\, dx \le \mathrm{TV}(u_0) = \int |u_0'(x)|\, dx$$

  The solution does not oscillate.
- Hyperbolic scaling: Space and time scale as $t \sim x$

$$u(x,t) = U(\xi(x,t)) \qquad \Longrightarrow \qquad u_t = U'\xi_t \sim u_x = U'\xi_x \qquad \Longrightarrow \qquad dt \sim dx$$

Parabolic Equations

$$\boxed{u_t - \nabla \cdot [D(u)\nabla u] = 0}$$

- Mass conservative
- Solutions smooth in time (the operator is compact on Sobolev spaces)

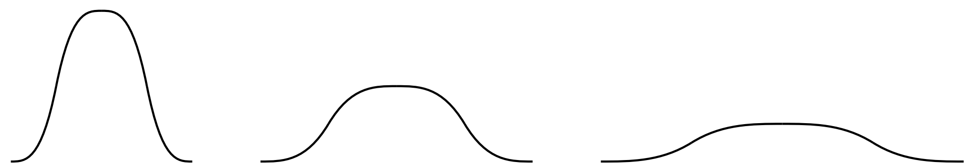

- Solutions are continuous. Initial discontinuities disappear immediately.
- The maximum principle: u is the average of nearby values.
  The solution does not oscillate.
- Parabolic scaling: Space and time scale as $t \sim x^2$

$$\begin{aligned} u(x,t) = U(\xi(x,t)) \qquad &\Longrightarrow \qquad u_t = U'\xi_t \sim u_{xx} = U'\xi_{xx} + U''(\xi_x)^2 \\ &\Longrightarrow \qquad dt \sim dx^2 \end{aligned}$$

Outline

1. The finite volume framework. Approximation requires
   - Reconstruction of the solution at points from average values
   - A time stepping method
2. Reconstruction: WENO with adaptive order (WENO-AO)
   - High order accurate when the solution is smooth
   - Reduce accuracy near shocks/steep fronts to suppress oscillations
3. Time stepping: method of lines
   - Implicit L-stable Runge-Kutta to handle stiffness (i.e., diffusion)
   - A new adaptive Runge-Kutta (high order Runge-Kutta combined with backward Euler) to further suppress oscillations
4. Numerical performance of iWENO-AO
5. Self-Adaptive Theta (SATh) scheme (a "better backward Euler")
   - Discontinuity Aware Quadrature (DAQ)
   - Theoretical Properties
6. Numerical performance of SATh-LF
7. Summary and conclusions

1. The Finite Volume Framework

Mass Conservation

- u is mass of a substance per unit volume (i.e., its density)
- $\mathbf{v}$ is the velocity of the substance
- E is a volume element
- $\int_E u(x,t)\,dx$ is the total mass in E

The change in mass is

$$\frac{d}{dt}\int_E u(x,t)\,dx \stackrel{?}{=} \int_E u_t(x,t)\,dx$$

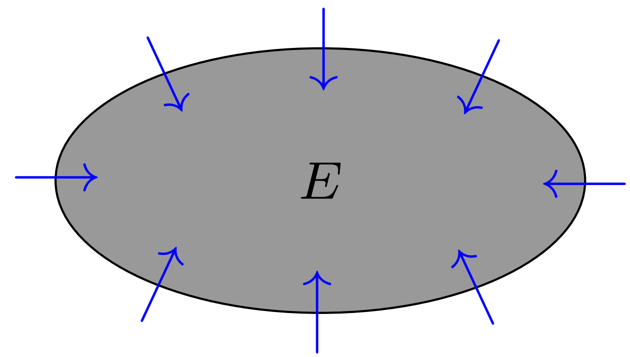

Changes are due to flow through ∂E:

$$-\int_{\partial E} \mathbf{v}(x,t)\cdot\nu\,d\sigma(x) = -\int_E \nabla\cdot\mathbf{v}(x,t)\,dx$$

by the Divergence Theorem. Equating, we have

$$\int_E \Big[u_t(x,t) + \nabla\cdot\mathbf{v}(x,t)\Big]dx = 0 \qquad \Longleftrightarrow \qquad u_t + \nabla\cdot\mathbf{v} = 0$$

since this is true for every measurable E

Empirical Constitutive Relation. How are u and $\mathbf{v}$ related? Assume

$$\mathbf{v} = f(u) - D(u)\nabla u$$

- Transport: motion due to the amount of material present u
- Diffusion: motion due to gradients in u

Finite volumes (mesh elements)

- Fix a computational mesh of polytopal elements E in $\mathbb{R}^d$
- The average of u over element E is

$$\bar{u}_E(t) = \frac{1}{|E|}\int_E u(x,t)\,dx$$

where $|E|$ is the d dimensional volume of E

The finite volume equation. Mass conservation over mesh element E:

$$\boxed{\bar{u}_{E,t} + \frac{1}{|E|}\int_{\partial E}\big(f(u) - D\nabla u\big)\cdot \nu_E\,d\sigma(x) = 0}$$

Introduce a Numerical Flux

A numerical flux function for the advective term is needed

- to stabilize the computations (by adding numerical diffusion)
- to account for potential discontinuities in the solution

Lax-Friedrichs numerical flux

$$\hat{f}_E(u^-, u^+) = \frac{1}{2}\Big[(f(u^-) + f(u^+)) \cdot \nu_E - \alpha_{\mathsf{LF}}(u^+ - u^-)\Big]$$

- u^- and u^+ are left and right limits of the solution at the interface ∂E
- $\alpha_{\mathsf{LF}} = \max_u \left|\partial f / \partial u\right|$
- if u is continuous, we have consistency with the original flux

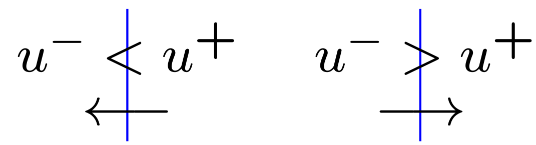

$$\hat{f}_E(u^-, u^+) = f(u) \cdot \nu_E$$

The averaged equation. Thus the advection-diffusion equation is

$$\boxed{\bar{u}_{E,t} + \frac{1}{|E|}\int_{\partial E} \hat{F}(u^-, u^+, \nabla u \cdot \nu_E)\, d\sigma(x) = 0}$$

where $\hat{F}_E(u-, u+, \nabla u \cdot \nu_E) = \hat{f}_E(u^-, u^+) - D\nabla u \cdot \nu_E$

Approximate integration.

- Let the facets of ∂E be denoted $e_1, e_2, \ldots$
- On each e_j, use a quadrature rule with points $x_{j,k}$ and weights $|e_j|\omega_{j,k}$
- Denote

$$u^{\pm}_{j,k}(t) = u^{\pm}(x_{j,k}, t) \approx u(x_{j,k}, t)$$
$$u_{j,k}(t) \approx u(x_{j,k}, t)$$

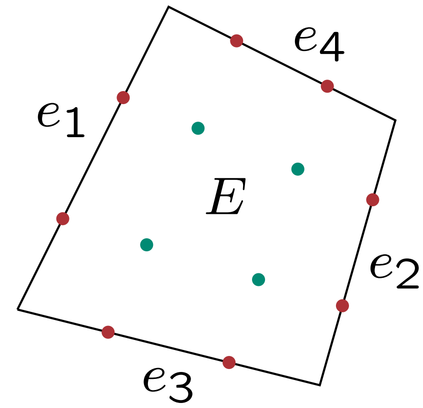

The semidiscrete finite volume approximation.

$$\boxed{\bar{u}_{E,t} + \sum_j \frac{|e_j|}{|E|} \sum_k \omega_{j,k} \widehat{F}_E(u^-_{j,k}, u^+_{j,k}, \nabla u \cdot \nu_E)_{j,k} = 0}$$

- Fix time levels $0 = t^0 < t^1 < t^2 < \cdots$
- We approximate $\bar{u}^n_E \approx \bar{u}_E(t^n)$ for each $n > 0$

Remaining Issues.

- Reconstruct $u^{\pm}_{j,k}$ and $(\nabla u \cdot \nu_E)_{j,k}$ from the discrete averages $\bar{u}^n_E$
- Define a fully discrete time evolution scheme

2. Reconstruction: Weighted Essentially Non-Oscillatory with Adaptive Order (WENO-AO)

For simplicity, reconstruct in 1D and
assume uniform meshes of spacing $\Delta x = h$

Classic ENO3 Reconstructions in 1D

(Harten, Engquist, Osher & Chakravarthy 1987)

Idea: Find a polynomial that reconstructs $u(x)$ from its average values. Shocks are isolated, so compute using several stencils.

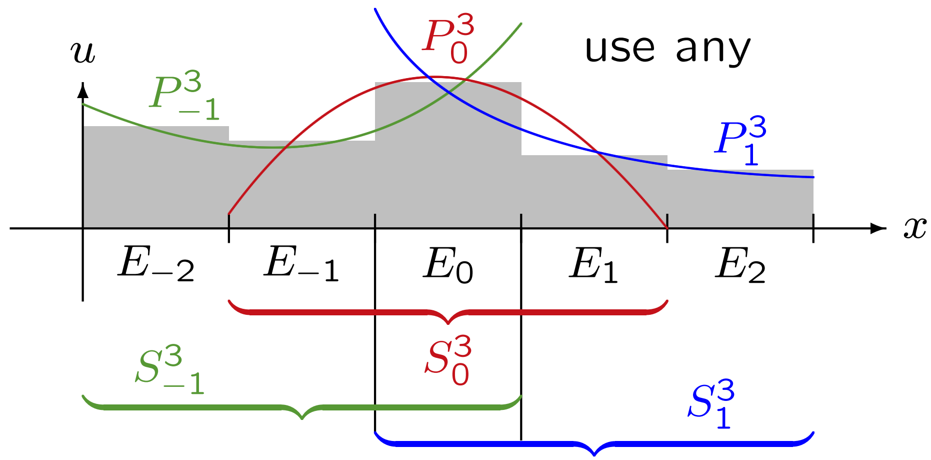

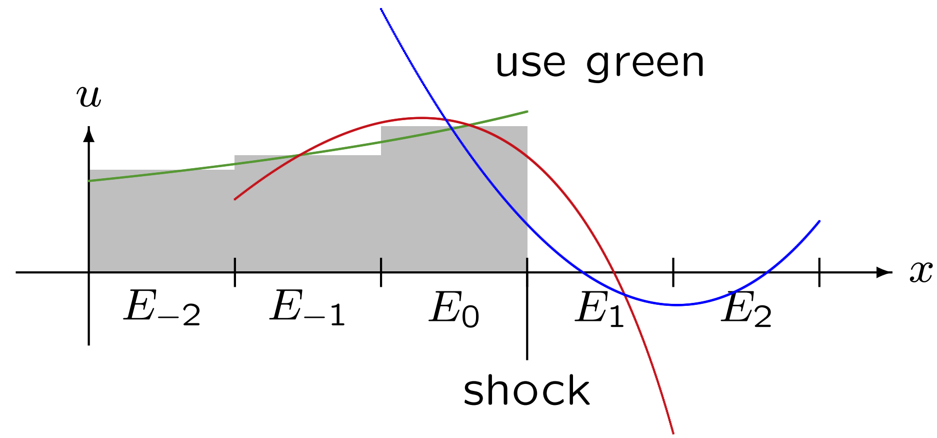

Find $P_i^3(x)$ of degree 2 so mass is conserved on each 3 element stencil

$$\frac{1}{h}\int_{E_j} P_i^3(x)\,dx = \bar{u}^n_{E_j} \quad (E_j \text{ in the stencil}) \quad \Longrightarrow \quad u(x) = P_i^3(x) + \mathcal{O}(h^3)$$

Use the "essentially non-oscillatory" polynomial not crossing the shock.

$$\boxed{u(x) \approx R(x) = P_i^3(x)} \quad \text{for some chosen } i,\ \mathcal{O}(h^3)$$

Problems

- Wasted stencil computations.
- Get a wide stencil.

Classic WENO3 Reconstructions in 1D

(Liu, Osher & Chan 1994; Jiang & Shu 1996)

Idea: Take a weighted average of smaller stencil polynomials that give the larger stencil polynomial.

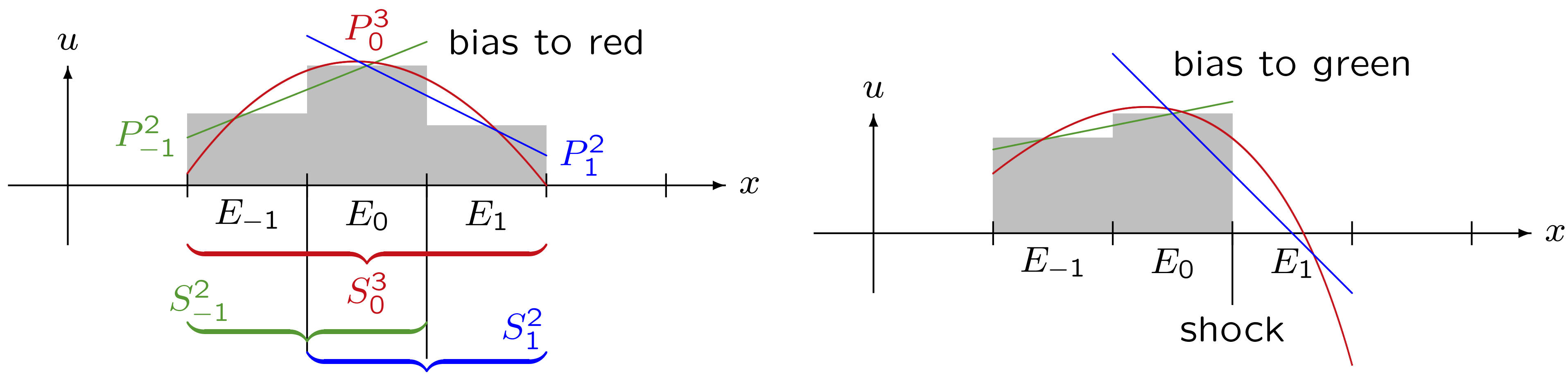

Find $P_i^2(x)$ of degree 1 so mass is conserved on small stencils ($\mathcal{O}(h^2)$)

For fixed x^*, define α, $\beta = 1 - \alpha$ so that

$$P_0^3(x^*) = \alpha P_{-1}^2(x^*) + \beta P_1^2(x^*) \qquad (\mathcal{O}(h^3) \text{ accurate})$$

and then modify the weights so

$$\boxed{u(x^*) \approx R(x^*) = \tilde{\alpha} P_{-1}^2(x^*) + \tilde{\beta} P_1^2(x^*)} \approx \begin{cases} P_{-1}^2(x^*) & \text{if shock right}, \mathcal{O}(h^2) \\ P_0^3(x^*) & \text{if no shock}, \mathcal{O}(h^3) \\ P_1^2(x^*) & \text{if shock left}, \mathcal{O}(h^2) \end{cases}$$

Problems

- The weights are difficult to find (not exist?!) and may be negative.
- Requires rectangular meshes in 2D/3D.

(Levy, Puppo & Russo 2000; Balsara, Garain & Shu 2016; Arbogast, Huang & Zhao 2018)

Idea: Use large and small stencil polynomials of different degrees.

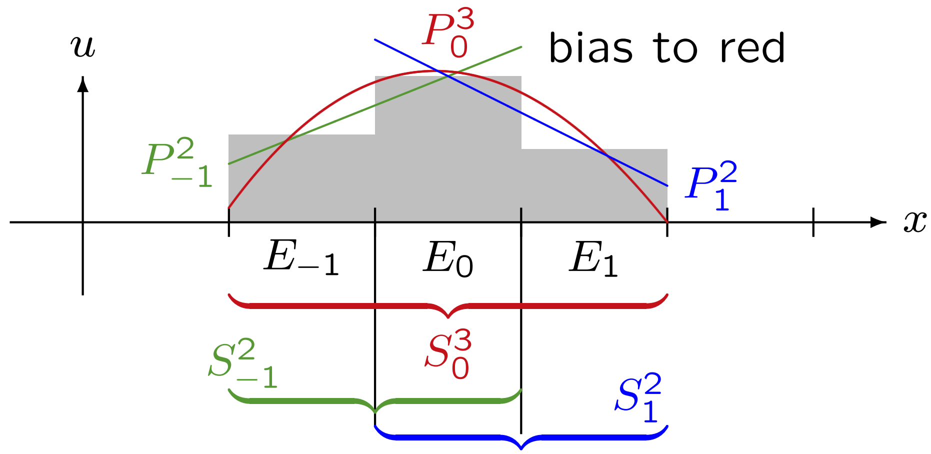

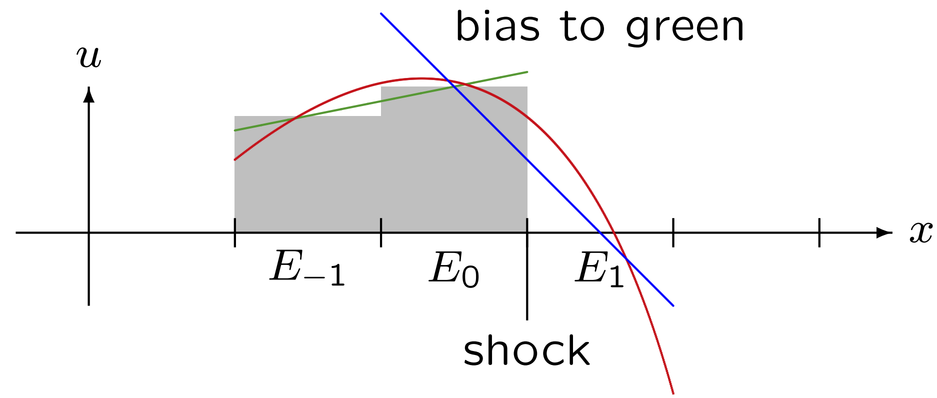

For *any* x, take *arbitrary* (positive) α, β, γ so that $\alpha+\beta+\gamma=1$

$$\boxed{u(x) \approx R(x) = \frac{\tilde\gamma}{\gamma}\Big[P_0^3(x) - \alpha P_{-1}^2(x) - \beta P_1^2(x)\Big] + \tilde\alpha P_{-1}^2(x) + \tilde\beta P_1^2(x)}$$

$$\approx \begin{cases} P_{-1}^2(x) & \text{if shock right, } \tilde\alpha\approx 1,\ \tilde\beta\approx 0,\ \tilde\gamma\approx 0,\ \mathcal{O}(h^2) \\ P_0^3(x) & \text{if no shock, } \tilde\alpha\approx\alpha,\ \tilde\beta\approx\beta,\ \tilde\gamma\approx\gamma,\ \mathcal{O}(h^3) \\ P_1^2(x) & \text{if shock left, } \tilde\alpha\approx 0,\ \tilde\beta\approx 1,\ \tilde\gamma\approx 0,\ \mathcal{O}(h^2) \end{cases}$$

Advantage

- Freedom from rectangular geometry (so extension to 2-D/3-D).

Smoothness indicator (Jiang & Shu 1996)

The smoothness (*roughness*) of $P^s(x)$ on E is measured as

$$\sigma_{P^s} = \sum_{\ell=1}^{s-1} \int_E h^{2\ell-1} \left(\frac{d^\ell}{dx^\ell} P^s(x) \right)^2 dx$$

- If u is smooth, $\sigma_{P^s} = Dh^2 + \mathcal{O}(h^3)$ $(D \approx u')$
- If u has a discontinuity, $\sigma_{P^s} = \mathcal{O}(1)$

Folklore. If u has a discontinuity, $\sigma_{P^s} = \Theta(1)$ as $h \to 0$ (i.e., $0 < c_* \le \sigma_{P^s} \le c* < \infty$).

Theorem (Arbogast, Huang & Zhao 2018)

If u has a discontinuity, σ_{P^s} may tend to zero as $h \to 0$. If the discontinuity is bounded away from the grid points, then $\sigma_{P^s} = \Theta(1)$.

Assumption. We will henceforth assume that the discontinuity is bounded away from the grid points, so $\sigma_{P^s} = \Theta(1)$.

Weighting Procedure — Nonlinear Weights

(Jiang & Shu 1996)

Scaled nonlinear weights. For weight δ for polynomial $P(x)$

$$\widehat{\delta} = \frac{\delta}{(\epsilon_h + \sigma_P)^\eta}$$

Classically, $\epsilon_h \approx 10^{-6}$, but $\epsilon_h = \epsilon_0 h^2$ should be taken.

(Normalized) Nonlinear weights. So that $\sum_i \tilde{\delta}_i = 1$,

$$\tilde{\delta}_i = \frac{\widehat{\delta}_i}{\sum_j \widehat{\delta}_j} = \frac{\delta_i}{\delta_i + \sum_{j \neq i} \delta_j \left(\dfrac{\epsilon_h + \sigma_{P_i}}{\epsilon_h + \sigma_{P_j}} \right)^\eta}$$

Lemma. (Aràndiga, Baeza, Belda & Mulet 2011)

$$\tilde{\delta} = \begin{cases} \delta + \mathcal{O}(h^{s-1}) & \text{if } u \text{ is smooth } (s \text{ is size of smaller stencil}) \\ \Theta(h^{2\eta}) & \text{if } u \text{ is discontinuous and } \epsilon_h = \epsilon_0 h^2 \end{cases}$$

General WENO-AO(r,s)

(Levy, Puppo & Russo 2000; Balsara, Garain & Shu 2016)

Idea: Use small stencils of s elements and the union (large stencil) of size r, with corresponding polynomials.

Take *arbitrary* (positive) γ and α_i, $\gamma + \sum_i \alpha_i = 1$

$$\boxed{u(x) \approx R(x) = \frac{\tilde{\gamma}}{\gamma}\Big[P_0^r(x) - \sum_i \alpha_i P_i^s(x)\Big] + \sum_i \tilde{\alpha}_i P_i^s(x)}$$

where

$$\hat{\gamma} = \frac{\gamma}{(\epsilon_h + \sigma_{P_0^r})^\eta} \qquad \hat{\alpha}_i = \frac{\alpha_i}{(\epsilon_h + \sigma_{P_i^s})^\eta}$$

$$\tilde{\gamma} = \frac{\hat{\gamma}}{\hat{\gamma} + \sum_i \hat{\alpha}_i} \qquad \tilde{\alpha}_i = \frac{\hat{\alpha}_i}{\hat{\gamma} + \sum_i \hat{\alpha}_i}$$

Question. Does it really work?

- When u is smooth, is R accurate to $\mathcal{O}(h^r)$?
- When u has a discontinuity on some (but not all) stencils, is R $\mathcal{O}(h^s)$?

Convergence Results for WENO-AO(r, s)

(Cravero, Puppo, Semplice & Visconti 2018; Arbogast, Huang & Zhao 2018)

$$\boxed{u(x) \approx R(x) = \frac{\tilde{\gamma}}{\gamma}\Big[P_0^r(x) - \sum_i \alpha_i P_i^s(x)\Big] + \sum_i \tilde{\alpha}_i P_i^s(x)}$$

Recall ϵ_0 and η: $\hat{\delta} = \dfrac{\delta}{(\epsilon_0 h^2 + \sigma)^\eta}$

Theorem. Let $\eta \geq 1$, $\epsilon_0 > 0$, and $r > s \geq 2$.
Then WENO-AO(r, s) has order of accuracy

- $\mathcal{O}(h^r)$ if u is smooth on the larger stencil S^r and

$$r \leq 2s - 1$$

- $\mathcal{O}(h^s)$ if u is smooth except for a jump discontinuity in some (but not all) stencils, the grids are bounded away from the discontinuity, and

$$\eta \geq s/2$$

(Arbogast, Huang & Zhao 2018)

There is a recursive, multilevel version WENO-AO$(r_\ell, r_{\ell-1}, \ldots, r_0 = s)$.

- $h = 0.1 \times 2^{-n}$
- $u(x) = x^3 + \sin(x) + H(x_* - x)$ (H is the Heaviside function)
- Shock location $x_* = -4h, -3h, -2h, -h$
- u is smooth only on stencils S^9, S^7, S^5, S^3, respectively
- set η based on the Theorem and $\epsilon_0 = 1$

Error and convergence rate of WENO-AO$(9,7,5,3)$ at $x = 0$

The convergence rate is indeed from the largest smooth stencil

	$x_* = -4h$		$x_* = -3h$		$x_* = -2h$		$x_* = -h$	
n	error	order	error	order	error	order	error	order
3	4.80E-19	9.01	6.03E-15	7.00	1.01E-10	5.01	7.88E-7	2.96
4	9.36E-22	9.00	4.72E-17	7.00	3.15E-12	5.00	1.00E-7	2.98
5	1.83E-24	9.00	3.69E-19	7.00	9.83E-14	5.00	1.26E-8	2.99
6	3.57E-27	9.00	2.89E-21	7.00	3.07E-15	5.00	1.58E-9	2.99
7	6.97E-30	9.00	2.26E-23	7.00	9.58E-17	5.00	1.98E-10	3.00
Expected order		9		7		5		3

- $h = 2^{-n}$
- $u(x) = H(-x)$ (H is the Heaviside function)
- $S^5 = \left\{[\frac{-3h}{2}, \frac{-h}{2}], [\frac{-h}{2}, \frac{h}{2}], [\frac{h}{2}, \frac{3h}{2}], [\frac{3h}{2}, \frac{5h}{2}], [\frac{5h}{2}, \frac{7h}{2}]\right\}$
- $\bar{u}_i = 1, 1/2, 0, 0, 0,$ respectively

WENO-AO$(5,3)$ error and convergence rate at $x = h/2$

The convergence rates are indeed $\Theta(h^{2\eta})$

	$\eta = 1$		$\eta = 1.5$		$\eta = 2$		$\eta = 3$	
n	error	order	error	order	error	order	error	order
6	8.58E-4	1.98	1.72E-5	3.00	4.07E-7	3.99	3.10E-10	5.99
7	2.15E-4	1.99	2.15E-6	3.00	2.55E-8	4.00	4.86E-12	6.00
8	5.39E-5	2.00	2.69E-7	3.00	1.59E-9	4.00	7.60E-14	6.00
9	1.35E-5	2.00	3.36E-8	3.00	9.95E-11	4.00	1.19E-15	6.00
Expected order		2		3		4		6

Remark: The good stencil polynomials are exact, so the rate is not limited to $\mathcal{O}(h^3)$.

Semidiscrete Third Order Advection-Diffusion in 1D

$$\boxed{\bar{u}_{i,t} + \frac{1}{h}\Big[\widehat{F}(u^-_{i+1/2}, u^+_{i+1/2}, u'_{i+1/2}) - \widehat{F}(u^-_{i-1/2}, u^+_{i-1/2}, u'_{i-1/2})\Big] = 0}$$

WENO-AO(3,2) for point values

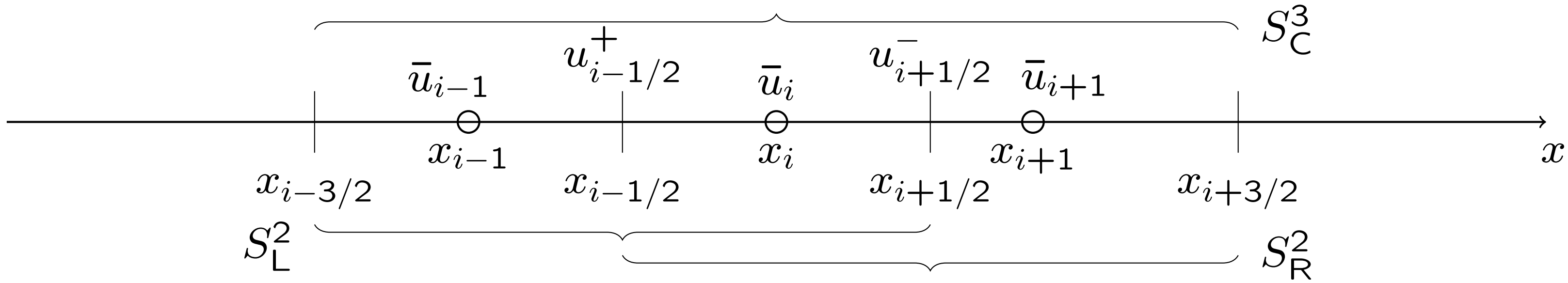

$$u(x) \approx R(x) = \frac{\tilde{\gamma}}{\gamma}\Big[P^3_{\mathsf{C}}(x) - \alpha P^2_{\mathsf{L}}(x) - \beta P^2_{\mathsf{R}}(x)\Big] + \tilde{\alpha} P^2_{\mathsf{L}}(x) + \tilde{\beta} P^2_{\mathsf{R}}(x)$$

$$u^+_{i-1/2} = R(x_{i-1/2}) \quad \text{and} \quad u^-_{i+1/2} = R(x_{i+1/2})$$

WENO-AO(4,3) for derivatives

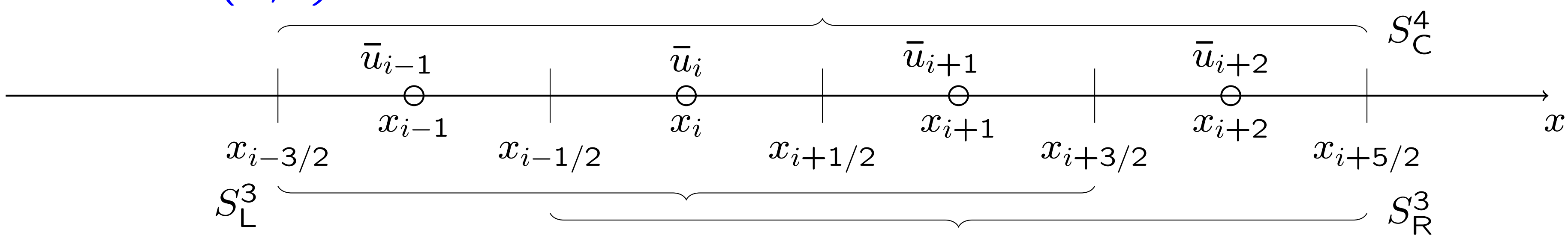

$$u'(x) \approx R'(x) = \frac{\tilde{\gamma}}{\gamma}\Big[P^{4\prime}_{\mathsf{C}}(x) - \alpha P^{3\prime}_{\mathsf{L}}(x) - \beta P^{3\prime}_{\mathsf{R}}(x)\Big] + \tilde{\alpha} P^{3\prime}_{\mathsf{L}}(x) + \tilde{\beta} P^{3\prime}_{\mathsf{R}}(x)$$

(maintains symmetry of the diffusion operator)

3. Time Stepping: Method of Lines

Use implicit Runge-Kutta methods
so $\Delta t \sim \Delta x$

- Δt_{CFL} is the time for fluid to move a distance Δx

$$\max |f'(u)| \, \Delta t_{\text{CFL}} = \Delta x$$

- The CFL number is

$$\text{CFL} = \frac{\Delta t}{\Delta t_{\text{CFL}}} \quad \begin{cases} \leq 1 & \text{fluid moves one cell per time step} \\ > 1 & \text{fluid moves many cells per time step} \end{cases}$$

- For explicit methods, stability requires
  - CFL ≤ 1
  - With diffusion, $\Delta t \sim \Delta x^2$ (parabolic scaling, i.e., stiffness)

Conclusion. We must do something!

- Operator splitting: split diffusion from advection (IMEX methods)
- Monolithic: Use fully implicit methods [we use this]

$$\boxed{\text{Choose } \Delta t \sim \Delta x \text{ for accuracy, not stability}}$$

Choice of Runge-Kutta Method

$$\frac{du}{dt} = G(u)$$

Strong-Stability Preserving (SSP) Runge-Kutta

- Preserves stability of backward Euler
- Requires CFL-like constraint for stability ($\Delta t \lessapprox \Delta t_{\mathsf{CFL}}$)
- Becomes unstable for large Δt

L-Stable Runge-Kutta

- Not SSP, but unconditionally stable
- Robust for stiff problems (e.g., with diffusion)
  - Stable: For $u' = au$ $(a < 0)$, $u^{n+1} = Q(\Delta t)u^n$ and $|Q(\Delta t)| \leq 1$.
  - L-Stable: Also $|Q(\Delta t)| \to 0$ as $\Delta t \to \infty$ (i.e., stable if Δt too large)

Radau IIA Runge-Kutta: 3rd order method:

$$u^{n+1/3} = u^n + \frac{\Delta t}{12}\left[5G(u^{n+1/3}) - G(u^{n+1})\right]$$

$$u^{n+1} = u^n + \frac{\Delta t}{4}\left[3G(u^{n+1/3}) + G(u^{n+1})\right]$$

Only two unknowns per mesh element (at times $t^{n+1/3}$ and t^{n+1})

Small Δt Radau IIA and SSP-RK perform similarly

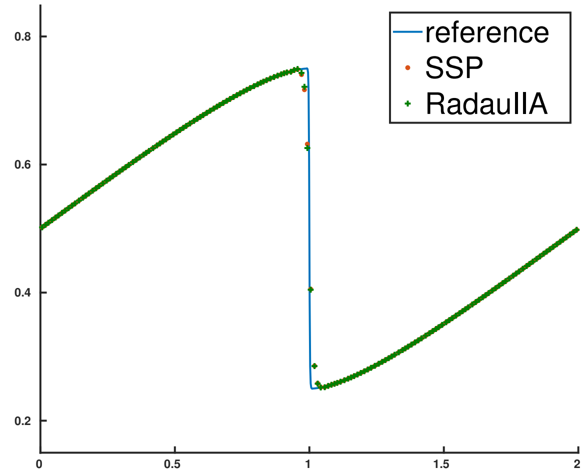

$\Delta t = 2\Delta x$

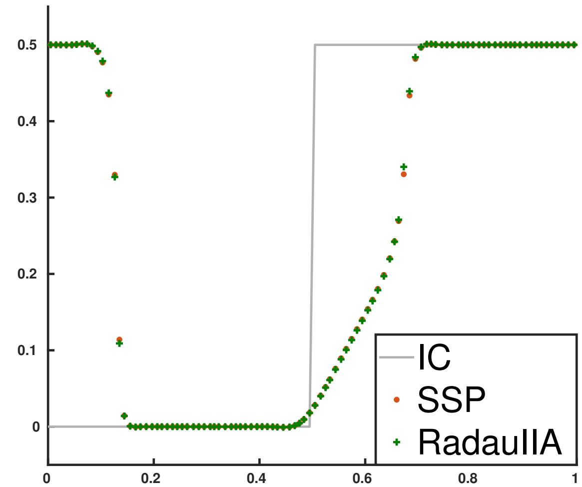

$\Delta t = 0.5\Delta x$

Large Δt Radau IIA overshoots a bit, SSP-RK is unstable

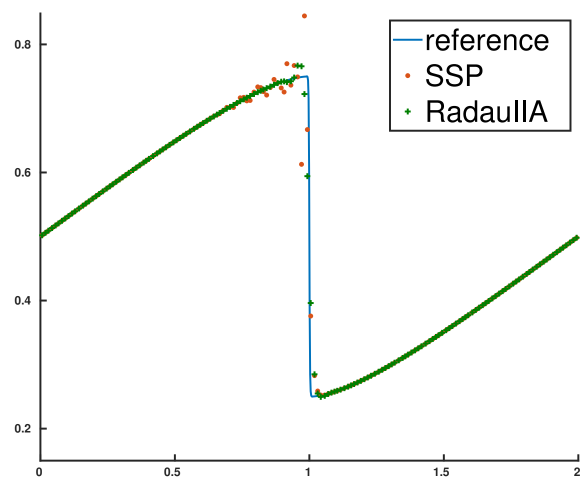

$\Delta t = 5\Delta x$

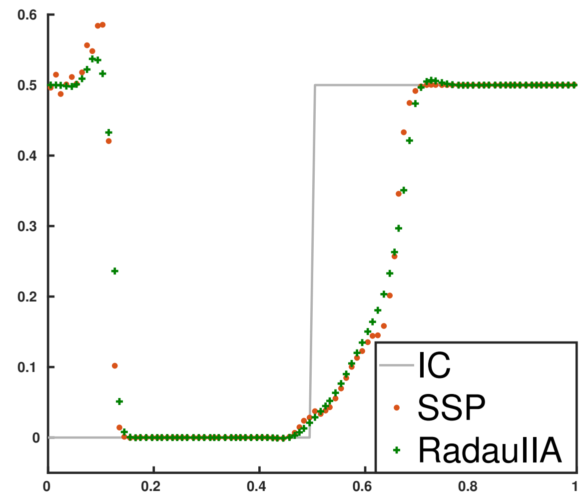

$\Delta t = 2\Delta x$

(Duraisamy, Baeder, Liu 2003; Ketcheson, MacDonald, Ruuth 2013; Arbogast, Huang, Zhao, King 2019)

Idea: Suppress the small oscillations near discontinuities by using

- Radau IIA Runge-Kutta when u is smooth
- composite backward Euler (BE) when u is discontinuous

Basically, we want

$$u^{n+1} \stackrel{?}{=} \tilde{w}^{\text{Radau}} u^{n+1,\text{Radau}} + \tilde{w}^{\text{BE}} u^{n+1,\text{BE}}$$

for some nonlinear weights $\tilde{w}^{\text{Radau}} + \tilde{w}^{\text{BE}} = 1$

Butcher Tableau: Gives the Runge-Kutta coefficients and time levels

$$\begin{array}{c|cc} 1/3 & 5/12 & -1/12 \\ 1 & 3/4 & 1/4 \\ \hline & 3/4 & 1/4 \end{array} \qquad \begin{array}{c|cc} 1/3 & 1/3 & 0 \\ 1 & 1/3 & 2/3 \\ \hline & 1/3 & 2/3 \end{array}$$

Radau IIA — composite BE

$$\begin{array}{c|cc} 1/3 & 5/12\tilde{w}^{\text{Radau}}+1/3\tilde{w}^{\text{BE}} & -1/12\tilde{w}^{\text{Radau}} \\ 1 & 3/4\tilde{w}^{\text{Radau}}+1/3\tilde{w}^{\text{BE}} & 1/4\tilde{w}^{\text{Radau}}+2/3\tilde{w}^{\text{BE}} \\ \hline & 3/4\tilde{w}^{\text{Radau}}+1/3\tilde{w}^{\text{BE}} & 1/4\tilde{w}^{\text{Radau}}+2/3\tilde{w}^{\text{BE}} \end{array}$$

adaptive Runge-Kutta

Application to Advection-Diffusion Equation in 1D

$$\boxed{\bar{u}_{i,t} + \frac{1}{h}\left[\widehat{F}_{i+1/2} - \widehat{F}_{i-1/2}\right] = 0}$$

- A conservative scheme requires unique fluxes at each grid point
- Apply the time-stepping to the flux at each grid point separately

$$\bar{u}_i^{n+1/3} = \bar{u}_i^n - \frac{\Delta t_n}{\Delta x_i}\Big[\tilde{a}^1_{i+1/2}\widehat{F}^{n+1/3}_{i+1/2} - \tilde{a}^1_{i-1/2}\widehat{F}^{n+1/3}_{i-1/2} + \tilde{a}^2_{i+1/2}\widehat{F}^{n+1}_{i+1/2} - \tilde{a}^2_{i-1/2}\widehat{F}^{n+1}_{i-1/2}\Big]$$

$$\bar{u}_i^{n+1} = \bar{u}_i^n - \frac{\Delta t_n}{\Delta x_i}\Big[\tilde{b}^1_{i+1/2}\widehat{F}^{n+1/3}_{i+1/2} - \tilde{b}^1_{i-1/2}\widehat{F}^{n+1/3}_{i-1/2} + \tilde{b}^2_{i+1/2}\widehat{F}^{n+1}_{i+1/2} - \tilde{b}^2_{i-1/2}\widehat{F}^{n+1}_{i-1/2}\Big]$$

where

$$\widehat{F}^{n+\theta}_{i\pm 1/2} = \widehat{F}(u^{n+\theta,-}_{i\pm 1/2}, u^{n+\theta,+}_{i\pm 1/2}, u'^{,n+\theta}_{i\pm 1/2}), \qquad \theta = 1/3, 1$$

$$\tilde{a}^1_{i\pm 1/2} = \frac{5}{12}\tilde{w}^{\text{Radau}}_{i\pm 1/2} + \frac{1}{3}\tilde{w}^{\text{BE}}_{i\pm 1/2} \qquad \tilde{a}^2_{i\pm 1/2} = -\frac{1}{12}\tilde{w}^{\text{Radau}}_{i\pm 1/2}$$

$$\tilde{b}^1_{i\pm 1/2} = \frac{3}{4}\tilde{w}^{\text{Radau}}_{i\pm 1/2} + \frac{1}{3}\tilde{w}^{\text{BE}}_{i\pm 1/2} \qquad \tilde{b}^2_{i\pm 1/2} = \frac{1}{4}\tilde{w}^{\text{Radau}}_{i\pm 1/2} + \frac{2}{3}\tilde{w}^{\text{BE}}_{i\pm 1/2}$$

Linear weighting

- BE is locally $\mathcal{O}(h^2)$ accurate, globally $\mathcal{O}(h)$ (for a smooth problem!)
- BE weight is $\boxed{w^{\text{BE}} = w_0^{\text{BE}} h^2}$ (or $w_0^{\text{BE}} \Delta t^2$, since $\Delta t \sim h$)
- Radau weight is $w^{\text{Radau}} = 1 - w^{\text{BE}}$.

Nonlinear weighting ($\eta \geq 1$ and $\epsilon_h = \epsilon_0 h^2$)

$$\widehat{w}_{i\pm1/2}^{\text{Radau}} = \frac{w^{\text{Radau}}}{(\epsilon_h + \sigma_{i\pm1/2}^{\text{Radau}})^\eta}, \qquad \widehat{w}_{i\pm1/2}^{\text{BE}} = \frac{w^{\text{BE}}}{(\epsilon_h + \sigma^{\text{BE}})^\eta},$$

$$\widetilde{w}_{i\pm1/2}^{\text{Radau}} = \frac{\widehat{w}_{i\pm1/2}^{\text{Radau}}}{\widehat{w}_{i\pm1/2}^{\text{BE}} + \widehat{w}_{i\pm1/2}^{\text{Radau}}}, \qquad \widetilde{w}_{i\pm1/2}^{\text{BE}} = 1 - \widetilde{w}_{i\pm1/2}^{\text{Radau}}.$$

Smoothness indicators (i.e., roughness)

- BE: $\boxed{\sigma^{\text{BE}} = 0}$ (BE can always be used)
- Radau: detect a shock in space

$$\sigma_{i\pm1/2}^{\text{Radau}} = \left(\bar{u}_{i\pm1}^n - \bar{u}_i^n\right)^2 + \left(\bar{u}_{i\pm1}^{n+1} - \bar{u}_i^{n+1}\right)^2 + \left(\bar{u}_{i\pm1}^{n+1/3} - \bar{u}_i^{n+1/3}\right)^2$$

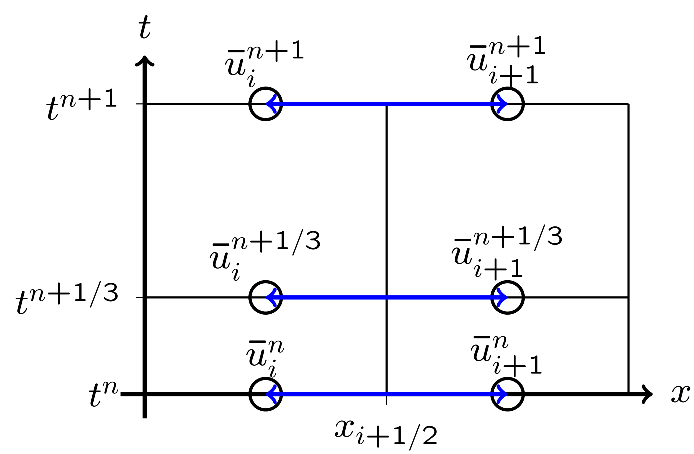

Consider the local time truncation error as a perturbation of Radau IIA.

Perturbed Radau weights

$$\tilde{a}^1_{i\pm1/2} = \frac{5}{12} - \frac{1}{12}\tilde{w}^{\mathrm{BE}}_{i\pm1/2} \qquad \tilde{a}^2_{i\pm1/2} = -\frac{1}{12} + \frac{1}{12}\tilde{w}^{\mathrm{BE}}_{i\pm1/2}$$
$$\tilde{b}^1_{i\pm1/2} = \frac{3}{4} - \frac{5}{12}\tilde{w}^{\mathrm{BE}}_{i\pm1/2} \qquad \tilde{b}^2_{i\pm1/2} = \frac{1}{4} + \frac{5}{12}\tilde{w}^{\mathrm{BE}}_{i\pm1/2}$$

Theorem. The adaptive Runge-Kutta scheme remains globally $\mathcal{O}(h^3)$ accurate when u is smooth. [Because $\omega^{\mathrm{BE}} = \mathcal{O}(h^2)$]

Numerical Test — Smooth Burgers' Equation

$$u_t + (u^2/2)_x = 0, \qquad x \in (0,2)$$
$$u(x,0) = \frac{1}{2}\left(1 - \frac{1}{2}\sin(\pi x)\right)$$

Error and convergence order at $T = 1$ (no shocks)

m	L_h^1 error	L_h^1 order	L_h^∞ error	L_h^∞ order
$\Delta t = h$				
640	3.21E-06	2.93	4.28E-05	2.87
1280	4.05E-07	2.99	5.47E-06	2.97
2560	5.07E-08	3.00	6.87E-07	2.99
$\Delta t = 10h$				
1280	1.86E-04	2.29	2.81E-03	1.92
2560	2.86E-05	2.70	4.84E-04	2.54
5120	3.78E-06	2.92	6.57E-05	2.88
$\Delta t = 50h$				
5120	3.09E-04	2.06	4.39E-03	1.67
10240	5.12E-05	2.59	8.45E-04	2.38
20480	7.13E-06	2.85	1.23E-04	2.78
	Expected	3		3

Analysis of Errors in Time — Discontinuous Case

Consider the local time truncation error (LTE) as a perturbation of BE.

Perturbed BE weights

$$\tilde{a}^1_{i\pm 1/2} = \frac{1}{3} + \frac{1}{12}\tilde{w}^{\text{Radau}}_{i\pm 1/2} \qquad \tilde{a}^2_{i\pm 1/2} = -\frac{1}{12}\tilde{w}^{\text{Radau}}_{i\pm 1/2}$$
$$\tilde{b}^1_{i\pm 1/2} = \frac{1}{3} + \frac{5}{12}\tilde{w}^{\text{Radau}}_{i\pm 1/2} \qquad \tilde{b}^2_{i\pm 1/2} = \frac{2}{3} - \frac{5}{12}\tilde{w}^{\text{Radau}}_{i\pm 1/2}$$

Conclusion. The LTE is formally the same as BE (i.e., $\mathcal{O}(h)$). However:

- BE should be $\mathcal{O}(h^{1/2})$ accurate with a discontinuity (LTE $= \mathcal{O}(h^{3/2})$).
- In practice, BE is $\mathcal{O}(h)$ accurate (LTE $= \mathcal{O}(h^2)$).

Numerical results show $\mathcal{O}(h)$ accuracy. Further investigation is underway.

Radau IIA and BE, $t = 2$, $m = 256$

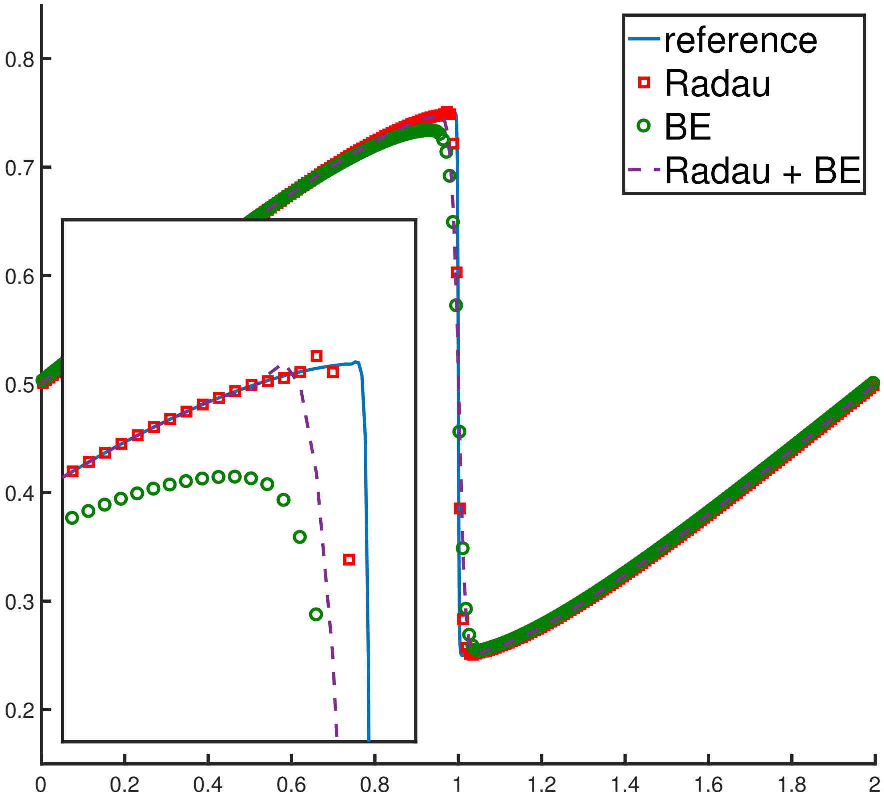

$\Delta t = 3h$

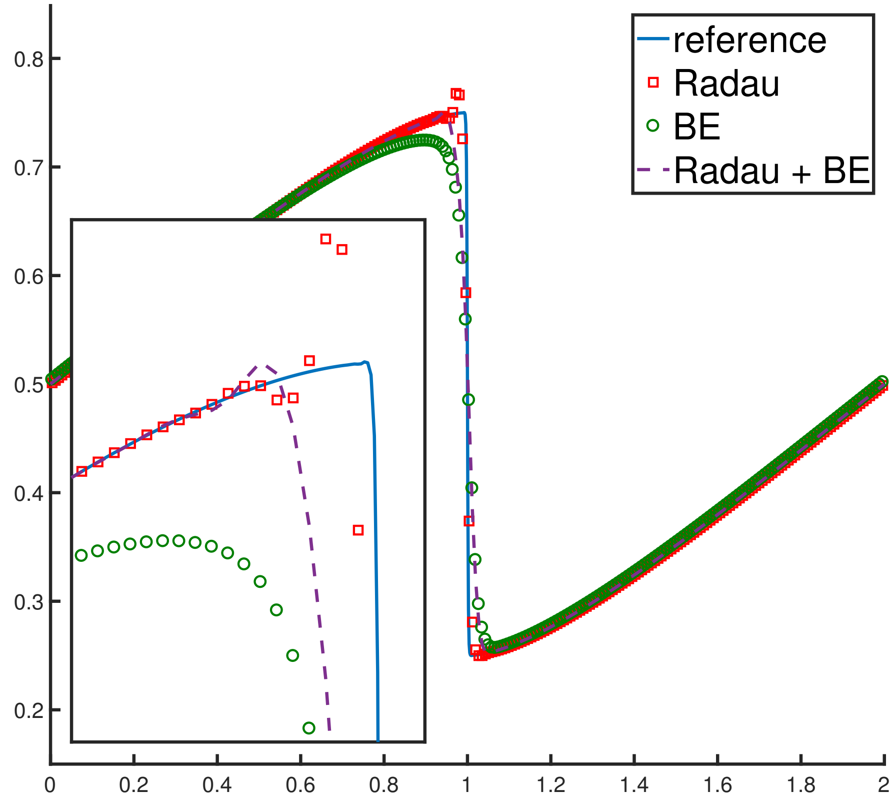

$\Delta t = 5h$

Remarks.

- The Radau overshoot is stable and does not grow.
- The adaptive scheme removes the oscillation and improves on BE.
- Away from the shock, the adaptive scheme is $\mathcal{O}(h^3)$ accurate.
- The SSP Runge-Kutta method is unstable at $\Delta t = 5h$.

Numerical Test — Burgers' Equation with Shock

$$u_t + (u^2/2)_x = 0, \quad x \in (0,2)$$
$$u(x,0) = 1 - H(x - 1/2) \quad (H \text{ is the Heaviside function})$$

Error and convergence order at $T = 1$ (initial shock)

	$\Delta t = 2h$		$\Delta t = 10h$	
m	L_h^1 error	order	L_h^1 error	order
	BE			
160	1.04E-02	0.98	2.73E-02	0.98
320	5.22E-03	0.99	1.37E-02	0.99
640	2.62E-03	1.00	6.86E-03	1.00
	Radau			
160	7.27E-03	1.00	1.70E-02	1.00
320	3.64E-03	1.00	8.47E-03	1.00
640	1.82E-03	1.00	4.23E-03	1.00
	Radau + BE			
160	1.03E-02	0.98	2.71E-02	0.97
320	5.19E-03	0.99	1.36E-02	0.99
640	2.60E-03	0.99	6.83E-03	1.00
	Expected?	1		1

Error and convergence order at $T = 1$ with $\Delta t = 10.5h$

m	L_h^1 error	L_h^1 order	L_h^∞ error	L_h^∞ order
		$D =$ 1E-01		
320	1.36E-04	2.56	1.19E-04	2.56
640	1.93E-05	2.82	1.67E-05	2.82
1280	2.50E-06	2.95	2.17E-06	2.95
		$D =$ 1E-02		
320	5.36E-08	2.97	6.15E-08	2.97
640	6.72E-09	2.99	7.72E-09	2.99
1280	8.47E-10	2.99	9.73E-10	2.99
		$D =$ 1E-04		
320	1.86E-12	2.96	4.20E-12	2.95
640	2.36E-13	2.98	5.33E-13	2.98
1280	2.96E-14	2.99	6.71E-14	2.99
	Expected	3		3

Remarks.

- Convergence is maintained as $D \to 0$

4. Numerical Performance of iWENO-AO

$$\frac{\partial u}{\partial t} + \frac{\partial u^2/2}{\partial x} + \frac{\partial u^2/2}{\partial y} - D\frac{\partial^2 u}{\partial x^2} = 0$$

We use randomly perturbed meshes of quadrilaterals in 2D

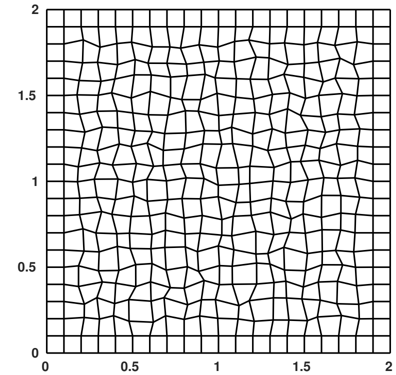

Error and convergence order for smooth solution at $t = 1$ using $\Delta t = 5h$ and quadrilateral meshes

m	$L^1_{\Delta x}$ -error	order	$L^\infty_{\Delta x}$-error	order
		$D = 0.1$		
20	3.254E-03	——	1.570E-03	——
40	4.908E-04	2.73	2.172E-04	2.85
80	6.687E-05	2.88	2.910E-05	2.90
160	8.742E-06	2.94	3.764E-06	2.95
		$D = 0.0001$		
20	2.023E-08	——	5.617E-08	——
40	5.705E-09	1.83	2.487E-08	1.18
80	1.058E-09	2.43	5.766E-09	2.11
160	1.330E-10	2.99	6.748E-10	3.10
	Expected	3		3

Numerical Test — Porous Medium Equation in 1D

$$\boxed{u_t = (u^m)_{xx} = \left((mu^{m-1})u_x\right)_x}$$

Barenblatt solution

$$B_m(x,t) = t^{-k}\left[\max\left(0, 1 - \frac{k(m-1)}{2m}\frac{|x|^2}{t^{2k}}\right)\right]^{1/(m-1)} \qquad k = \frac{1}{m+1}, \quad m > 1$$

This solution has compact support $[-\alpha_m(t), \alpha_m(t)]$, where

$$\alpha_m(t) = \sqrt{\frac{2m}{k(m-1)}}\, t^k$$

Non-uniform mesh of 120 elements at $t = 2$ (from $t = 1$), $\Delta t = h$

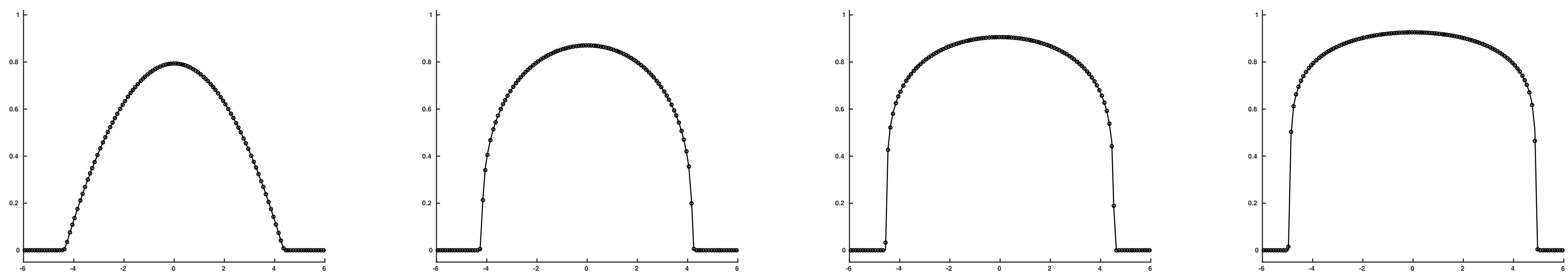

$m = 2$ $\quad$ $m = 4$ $\quad$ $m = 6$ $\quad$ $m = 8$

Quarter 5 spot pattern of petroleum wells

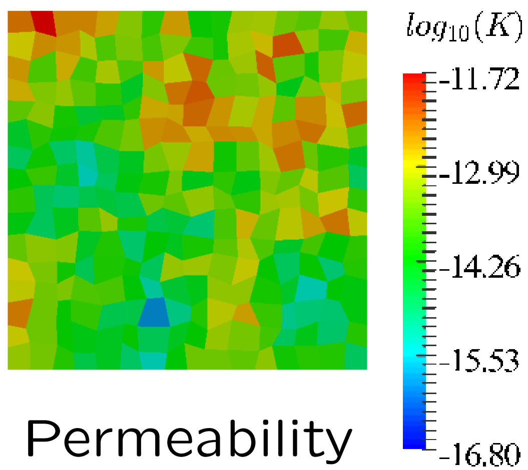

Permeability on Quadrilateral Mesh

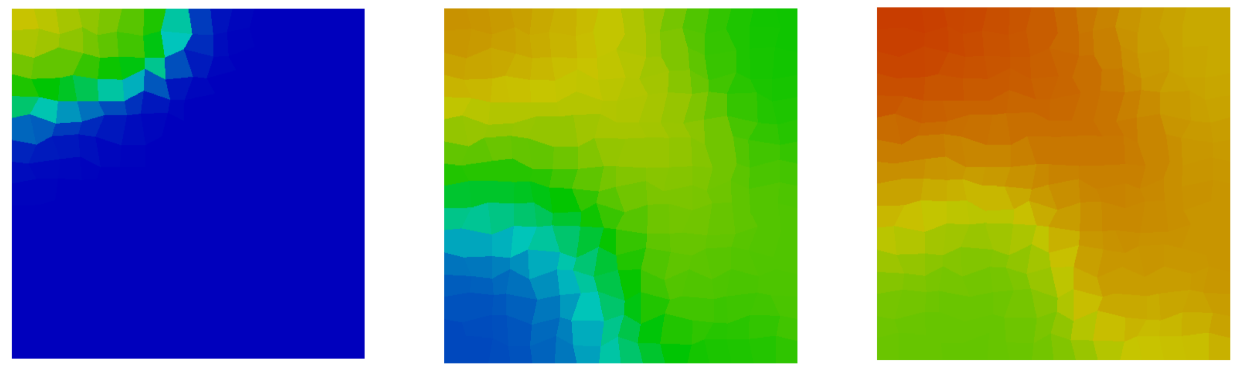

$t = 5$ days $t = 50$ days $t = 455$ days

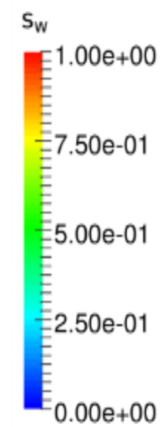

Undershoot wave: -3.14E-4

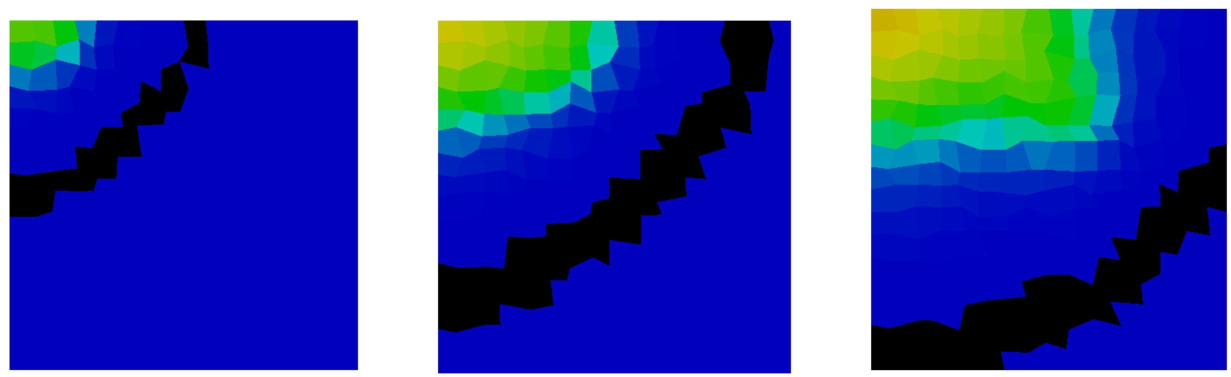

$t = 1$ day $t = 10$ days $t = 15$ days

Some small undershoots, but essentially non-oscillatory

Extensions. Easily extends to:

- higher order schemes;
- 3D on general computational meshes;
- systems of equations.

Efficiency.

- Uses 2 unknowns per mesh element per system component, independent of the space dimension! (For third order Radau IIA)
- Can use very long time steps, and $\Delta t \sim h$, not h^2.
- Reconstruction boosts parallel computing (less data transfer, more local computation)

Numerical Accuracy.

- Formal accuracy is $\mathcal{O}(h^3 + \Delta t^3)$ for smooth solutions.
- Essentially non oscillatory.
- The scheme is unconditionally von Neumann (Fourier) L-stable for smooth solutions to the linear problem.

Physical Accuracy.

- Locally mass conservative at $t^{n+1/3}$ and t^{n+1}.
- Handles both advection and diffusion (even $D = 0$).

5. A Self-Adaptive Theta Scheme (SATh)

Replace backward Euler
in the adaptive time stepping

Notation:

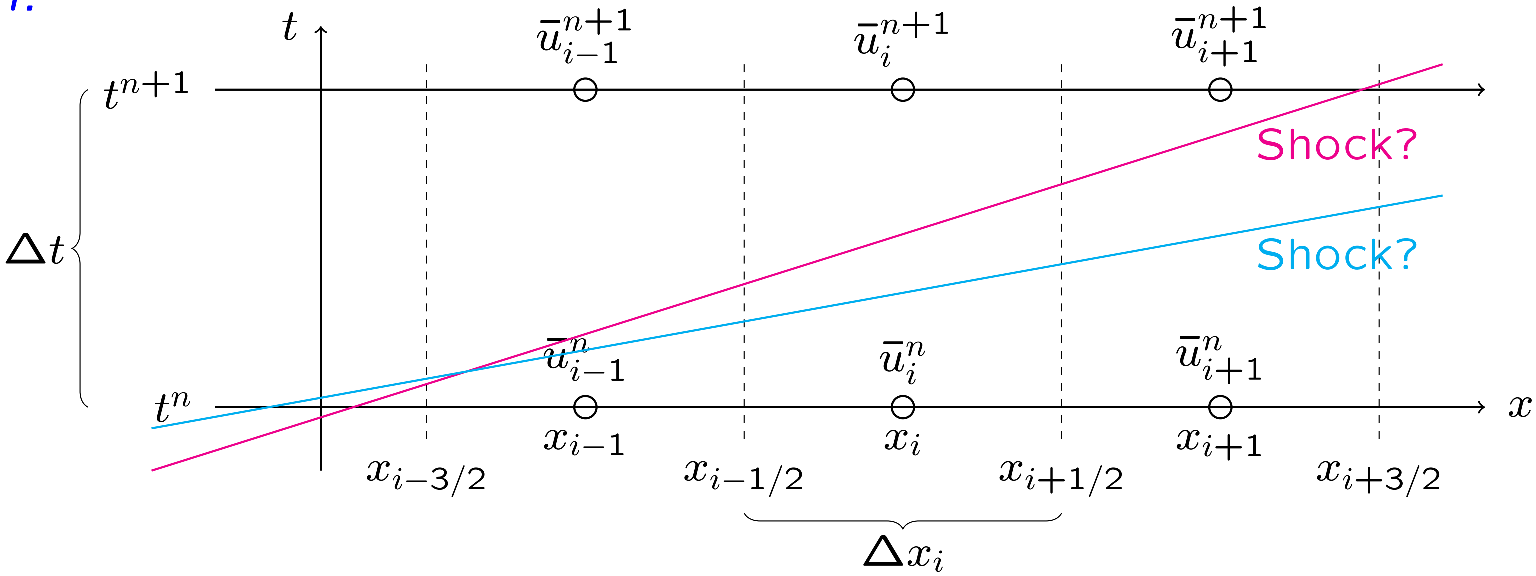

Basic equation 1. The governing equation directly controls $\bar{u}_i^{n+1}$.

$$\boxed{\bar{u}_i^{n+1} = \bar{u}_i^n - \frac{1}{\Delta x_i} \int_{t^n}^{t^{n+1}} \left[f(u_{i+1/2}(t)) - f(u_{i-1/2}(t)) \right] dt}$$

Problem. A shock in space is also a shock in time!
Using only $\bar{u}_i^n$ and $\bar{u}_i^{n+1}$ (and nearest neighbors), we cannot tell where the shock is in time.

Requirement. We need information over the entire time interval!

Notation:

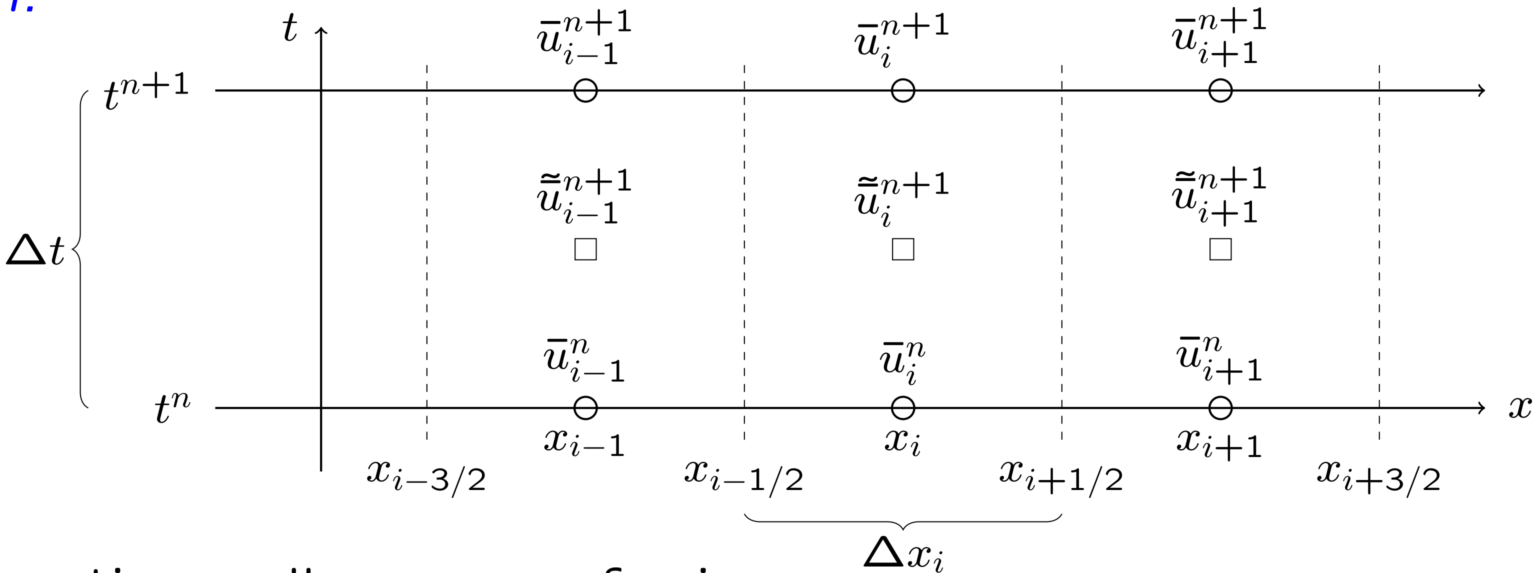

The space-time cell average of u is

$$\tilde{\bar{u}}_i^{n+1} = \frac{1}{\Delta t \Delta x_i} \int_{t^n}^{t^{n+1}} \int_{x_{i-1/2}}^{x_{i+1/2}} u(x,t)\, dx\, dt$$

Fact. The governing equation directly controls $\tilde{\bar{u}}_i^{n+1}$!

Basic equation 2. We use a test function $w(t) = (t^{n+1} - t)/\Delta t$ to see

$$\int_{t^n}^{t^{n+1}} \bar{u}_i'(t)\, w(t)\, dt = \bar{u}_i(t)\, w(t)\Big|_{t^n}^{t^{n+1}} - \int_{t^n}^{t^{n+1}} \bar{u}_i(t)\, w'(t)\, dt$$
$$= -\bar{u}_i^n + \tilde{\bar{u}}_i^{n+1}$$

Then

$$\int_{t^n}^{t^{n+1}} \int_{x_{i-1/2}}^{x_{i+1/2}} \Big(u_t + f(u)_x\Big)\, w(t)\, dx\, dt = 0$$

$\Longrightarrow$

$$\boxed{\tilde{\bar{u}}_i^{n+1} = \bar{u}_i^n - \frac{1}{\Delta t \Delta x_i} \int_{t^n}^{t^{n+1}} \Big(f(u_{i+1/2}) - f(u_{i-1/2})\Big)(t^{n+1} - t)\, dt}$$

5.1. Discontinuity Aware Quadrature (DAQ)

Problem description. Accurately approximate

$$\int_0^{\Delta t} g(v(t))\, w(t)\, dt$$

- g and w are smooth
- $v(t)$ is smooth except for a discontinuity at $0 \le \tau \le \Delta t$

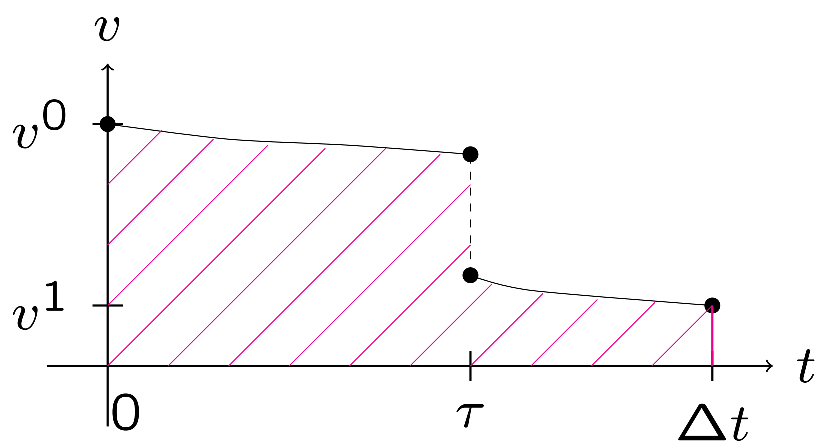

Use only the data

$$v^0 = v(0) \qquad v^1 = v(\Delta t) \qquad \tilde{v} = \frac{1}{\Delta t}\int_0^{\Delta t} v(t)\, dt$$

Idealize the picture.

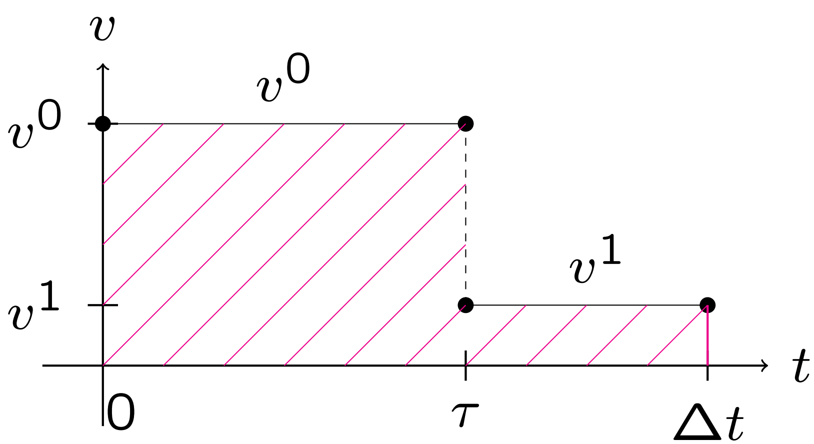

$$\tilde{v} = \frac{1}{\Delta t}\Big[\tau v^0 + (1-\tau)v^1\Big] \qquad \Longrightarrow \qquad \tau = \frac{v^1 - \tilde{v}}{v^1 - v^0}\Delta t$$

DAQ approximation.

$$\boxed{\int_0^{\Delta t} g(v(t))\, w(t)\, dt \approx g(v^0) \int_0^{\tau} w(t)\, dt + g(v^1) \int_{\tau}^{\Delta t} w(t)\, dt}$$

Application. Let $\theta = 1 - \dfrac{\tau}{\Delta t} = \dfrac{\tilde{v} - v^0}{v^1 - v^0}$

$$w = 1 \qquad \int_0^{\Delta t} g(v(t))\, dt \approx \Big[g(v^0) + \theta\Big((g(v^1) - g(v^0))\Big)\Big]\Delta t$$

$$w = \frac{t^1 - t}{\Delta t} \qquad \int_0^{\Delta t} g(v(t))\, w(t)\, dt \approx \frac{1}{2}\Big[g(v^0) + \theta^2\Big((g(v^1) - g(v^0))\Big)\Big]\Delta t$$

5.2. Application to Finite Volume Schemes

Monotone flux. Suppose that $f'(u) > 0$.

- Use one-point upstream weighting to stabilize the scheme
- Let $\bar{f}_i^n = f(\bar{u}_i^n)$

The upstream-weighted scheme. (SATh-up)

$$\bar{u}_i^{n+1} = \bar{u}_i^n - \frac{\Delta t}{\Delta x_i}\Big[\bar{f}_i^n + \theta_i(\bar{f}_i^{n+1} - \bar{f}_i^n) - \bar{f}_{i-1}^n - \theta_{i-1}(\bar{f}_{i-1}^{n+1} - \bar{f}_{i-1}^n)\Big]$$

$$\tilde{\bar{u}}_i^{n+1} = \bar{u}_i^n - \frac{\Delta t}{2\Delta x_i}\Big[\bar{f}_i^n + \theta_i^2(\bar{f}_i^{n+1} - \bar{f}_i^n) - \bar{f}_{i-1}^n - \theta_{i-1}^2(\bar{f}_{i-1}^{n+1} - \bar{f}_{i-1}^n)\Big]$$

where

$$\theta_i = \begin{cases} \max\left(\dfrac{1}{2}, \dfrac{\tilde{\bar{u}}_i^{n+1} - \bar{u}_i^n}{\bar{u}_i^{n+1} - \bar{u}_i^n}\right) & \text{if } |\bar{u}_i^{n+1} - \bar{u}_i^n| > \epsilon \\ \theta^* & \text{if } |\bar{u}_i^{n+1} - \bar{u}_i^n| \le \epsilon \end{cases}$$

- $\epsilon \ge 0$ is very small (even zero)
- $\theta^* = 1$ (backward Euler) or possibly $\theta^* = 1/2$ (Crank-Nicolson)

This is a self-adaptive theta method!

Remark. A Lax-Friedrichs stabilized SATh-LF scheme is similar.

$$u_t + u_x = 0 \quad \text{for } 0 < x < 1$$

$\Delta x = 1/100$, $\Delta t = 1/20$ (CFL = 5), $t = 0.5$ (10 steps)

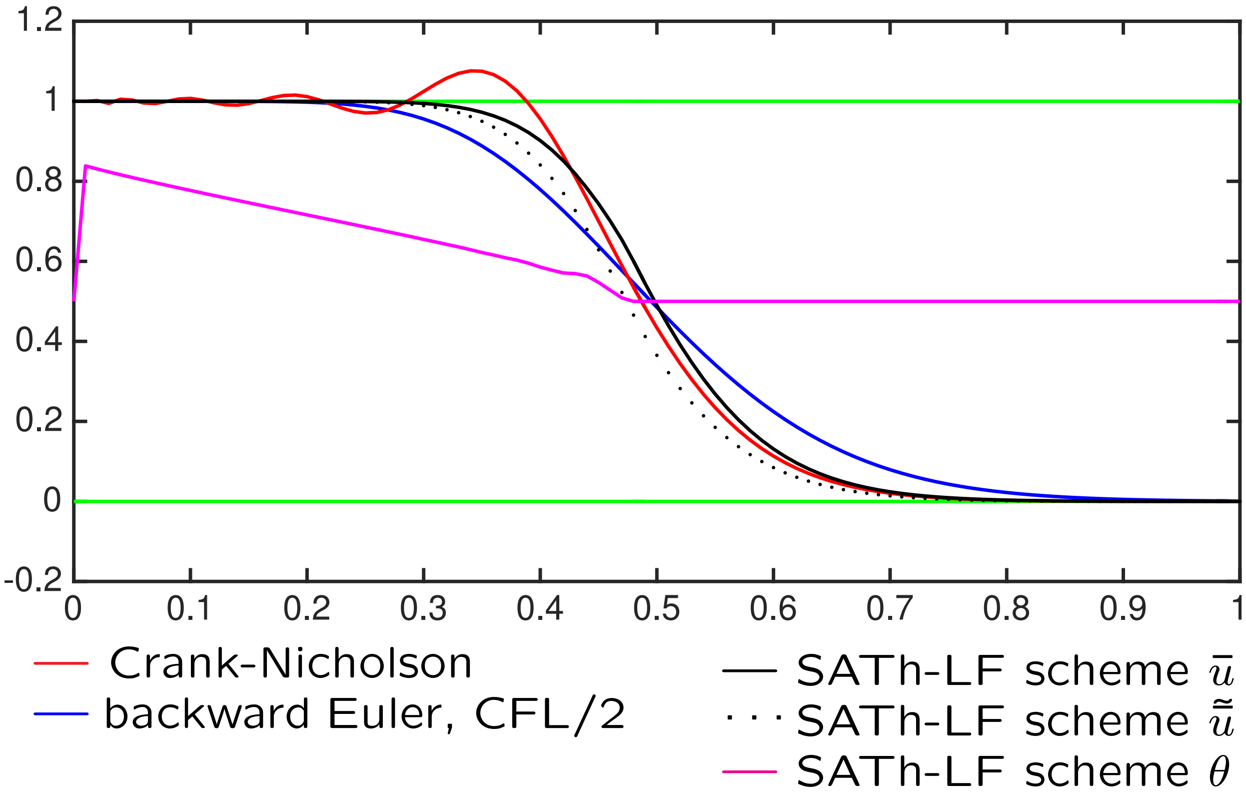

m	$L^1_{\Delta x}$ error	order
10	1.95E-1	——
20	1.53E-1	0.35
40	1.10E-1	0.48
80	7.56E-2	0.54
160	5.17E-2	0.55
320	3.54E-2	0.55

5.3. Theoretical Properties of SATh

Theorem. Let $g(v)$ be a smooth function and $v(t)$ satisfy the conditions for an isolated discontinuity at $\tau \in (0, \Delta t)$. If τ^* is the approximation to τ, then

$$|\tau - \tau^*| \le C\Delta t^2$$

$$\left| \int_0^{\Delta t} g(v(t))\, w(t)\, dt - \mathrm{DAQ}(gw) \right| \le C\Delta t^2$$

where C depends only on the L^∞ norms of g', w, v'_L, and v'_R

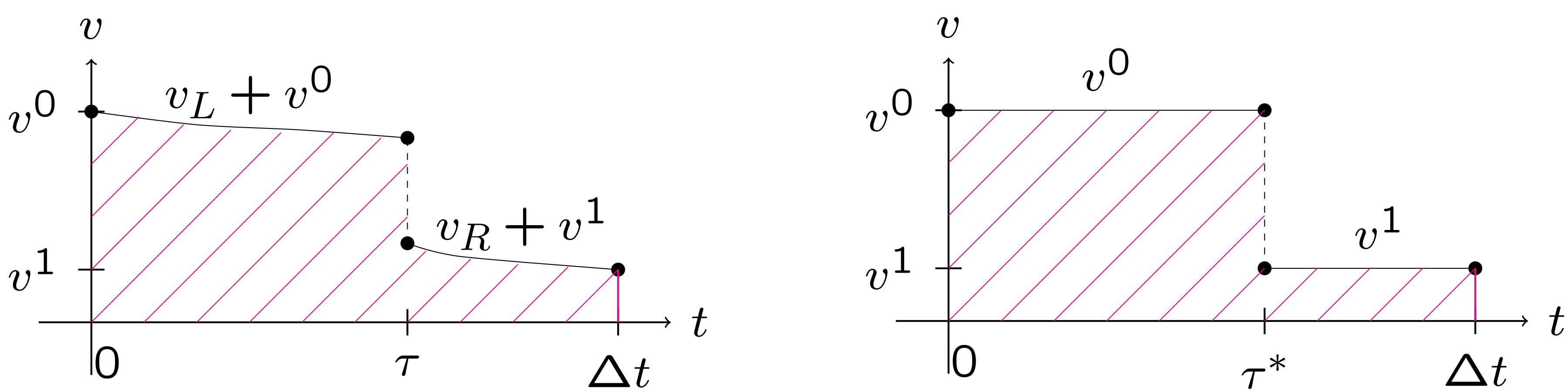

Consequence. The local truncation error is $\mathcal{O}(\Delta t^2)$.

$$\boxed{\text{The scheme should be } \mathcal{O}(\Delta x + \Delta t)}$$

Stability of the Upstream-Weighted Scheme

Theorem. Assume that

- $f(0) = 0$ and $f'(u) > 0$ for $u \neq 0$
- the problem has a boundary condition imposed on the left

The upstream weighted scheme (SATh-up) is unconditionally stable for the nonlinear problem if

$$\theta_i \geq \frac{1}{2}$$

Maximum Principle for the Upstream-Weighted Scheme

Theorem. For the upstream weighted scheme (SATh-up), assume

- $f = f(u)$ only, $f'(u) > 0$ and $\epsilon = 0$ (in defining θ_i)
- the problem has a boundary condition on the left (so $\bar{u}_0^n$ is given)

If the IC and BC of the flow is monotonically decreasing,

$$\bar{u}_{i-1}^0 \geq \bar{u}_i^0 \quad \text{and} \quad \bar{u}_0^n \leq \bar{u}_0^{n+1} \qquad \text{then} \qquad \bar{u}_i^n \leq \bar{u}_i^{n+1} \leq \bar{u}_{i-1}^{n+1}$$

If the IC and BC of the flow is monotonically increasing,

$$\bar{u}_{i-1}^0 \leq \bar{u}_i^0 \quad \text{and} \quad \bar{u}_0^n \geq \bar{u}_0^{n+1} \qquad \text{then} \qquad \bar{u}_i^n \geq \bar{u}_i^{n+1} \geq \bar{u}_{i-1}^{n+1}$$

Moreover,

- If $\tilde{\bar{u}}_0^{n+1}$ lies between $\bar{u}_0^n$ and $\bar{u}_0^{n+1}$, then $1/2 \leq \theta_i \leq 1$
- If $\theta^* = 1$ (in defining θ_i), then $\tilde{\bar{u}}_i^{n+1}$ lies between $\bar{u}_i^n$ and $\bar{u}_i^{n+1}$

Corollary. The Total Variation

$$\mathrm{TV}(\bar{u}^n) = \sum_{i=1}^{\infty} |\bar{u}_{i-1}^n - \bar{u}_i^n|$$

is bounded (TVB) and diminishes (TVD) under appropriate hypotheses

6. Numerical Performance of SATh-LF

Burgers Equation, Riemann Shock

$$u_t + (u^2/2)_x = 0 \quad \text{for } 0 < x < 1$$

$$\Delta x = 1/80,\ \Delta t = 1/16\ (\mathrm{CFL} = 5),\ t = 1.0$$

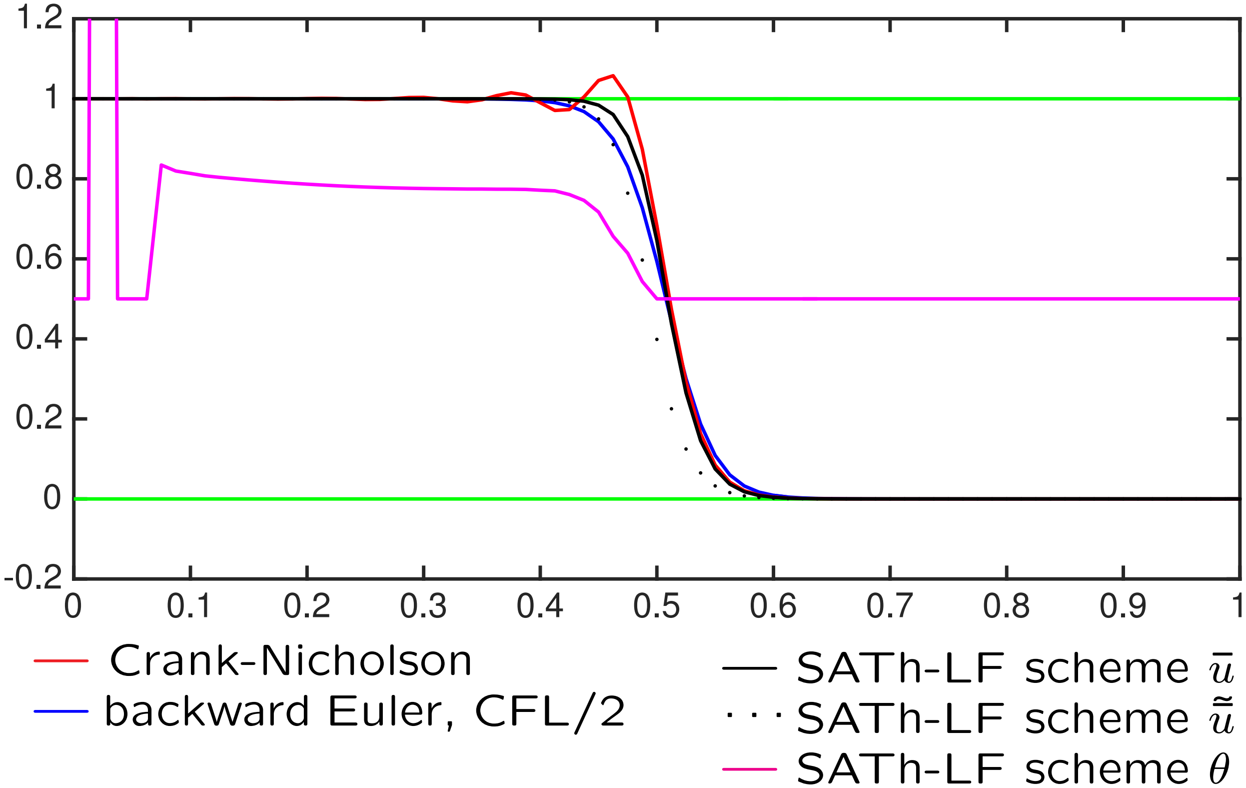

m	$L^1_{\Delta x}$ error	order
10	1.76E-1	——
20	9.74E-2	0.86
40	4.97E-2	0.97
80	2.49E-2	1.00
160	1.24E-2	1.00
320	6.22E-3	1.00

Burgers Equation, Riemann Rarefaction

$$u_t + (u^2/2)_x = 0 \quad \text{for } 0 < x < 1$$

$$\Delta x = 1/80,\ \Delta t = 1/16\ (\text{CFL} = 5),\ t = 0.25$$

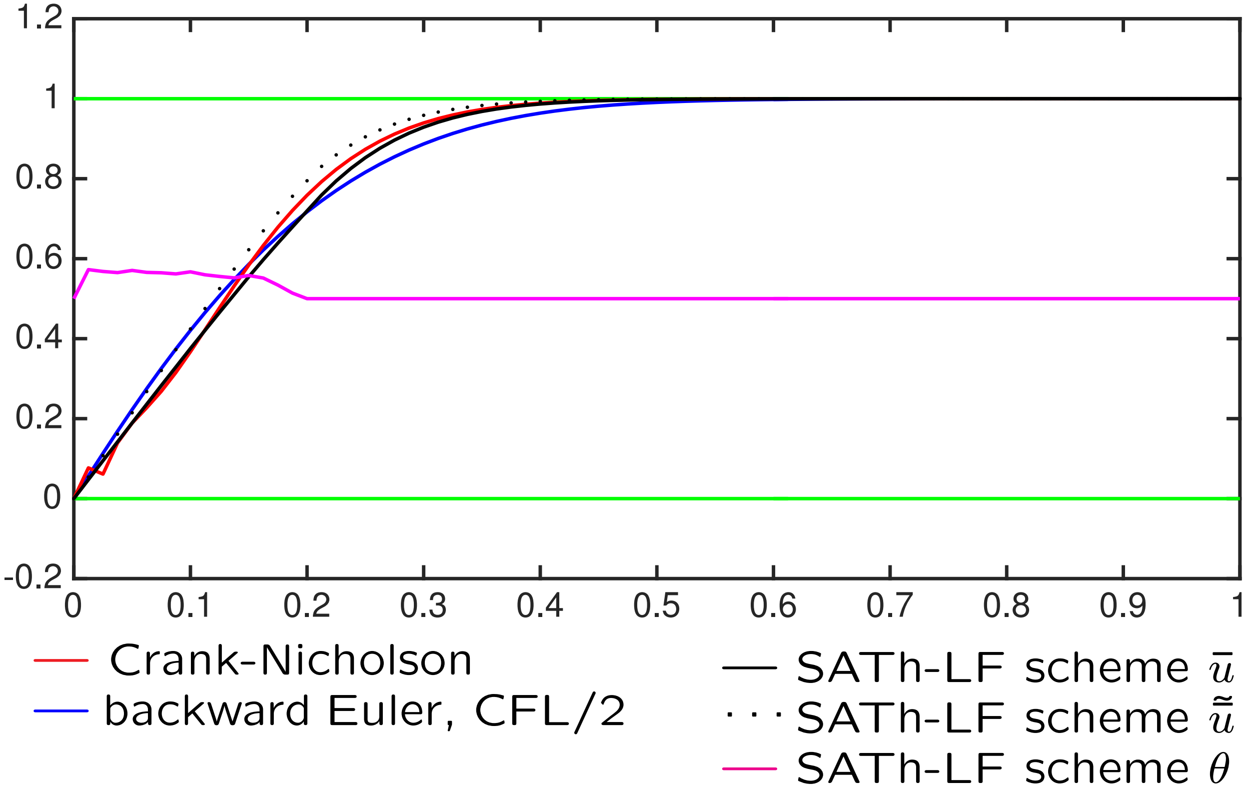

m	$L^1_{\Delta x}$ error	order
20	7.88E-2	——
40	4.66E-2	0.76
80	2.72E-2	0.78
160	1.56E-2	0.80
320	8.86E-3	0.82
640	4.96E-3	0.84

Burgers Equation, Shock formation

$$u_t + (u^2/2)_x = 0 \quad \text{for } 0 < x < 1$$

$$\Delta x = 1/160,\ \Delta t = 1/24\ (\text{CFL} = 4)$$

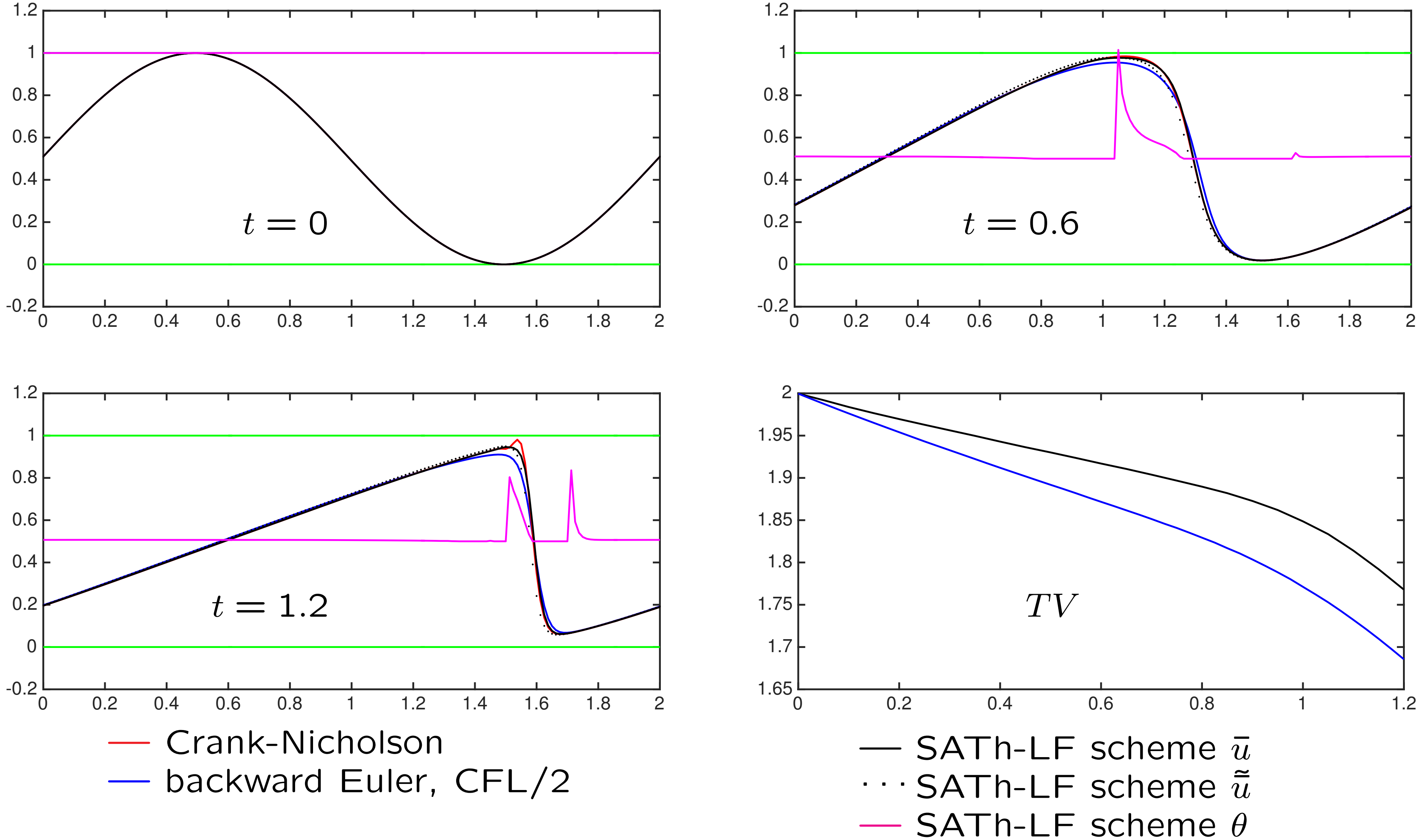

Buckley-Leverett Equation, Rarefaction and Shock

$$u_t + \left(u^2/(u^2+(1-u)^2)\right)_x = 0 \quad \text{for } 0 < x < 1$$

$$\alpha_{\mathrm{LF}} = 2,\ t = 0.5$$

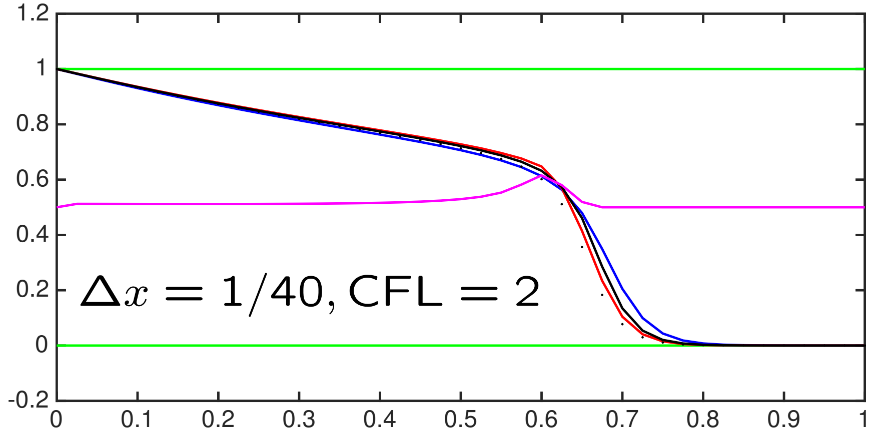

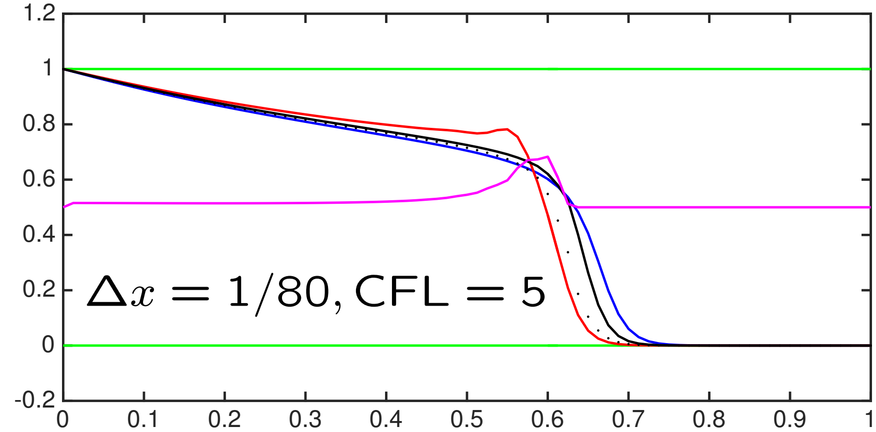

Crank-Nicholson
backward Euler, CFL/2

SATh-LF scheme $\bar{u}$
SATh-LF scheme $\tilde{\bar{u}}$
SATh-LF scheme θ

A Non Monotone Flux Function, Step Down

$$u_t + f(u)_x = 0 \quad \text{for } 0 < x < 1$$

$$\alpha_{\mathsf{LF}} = 1$$

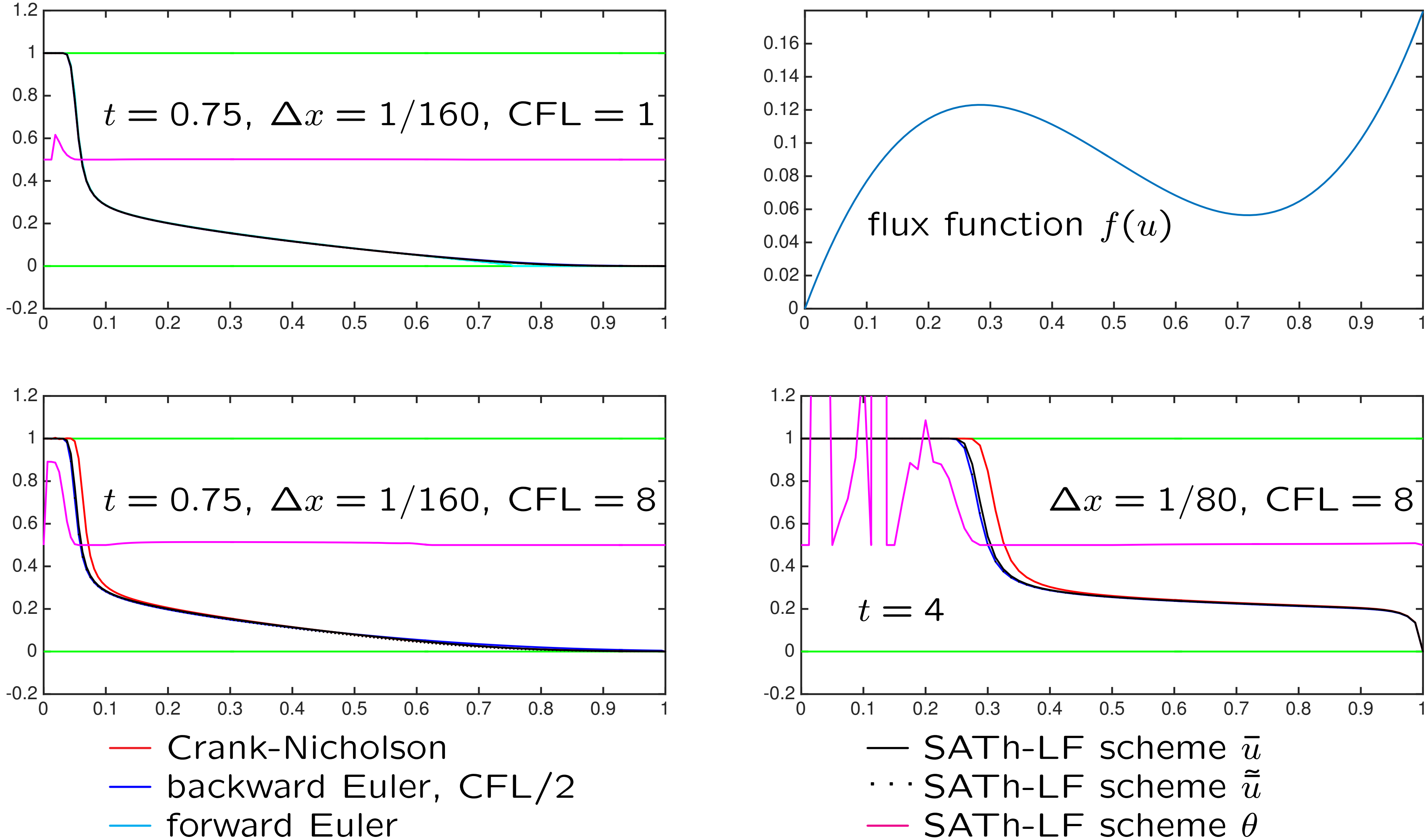

Burgers Equation in 2D

$$u_t + (u^2/2)_x + (u^2/2)_y = 0 \quad \text{for } 0 < x < 1, 0 < y < 1$$

$$\Delta x = \Delta y = 1/40,\ \Delta t = 1/10\ (\text{CFL} = 4),\ \alpha_{\text{LF}} = 1$$

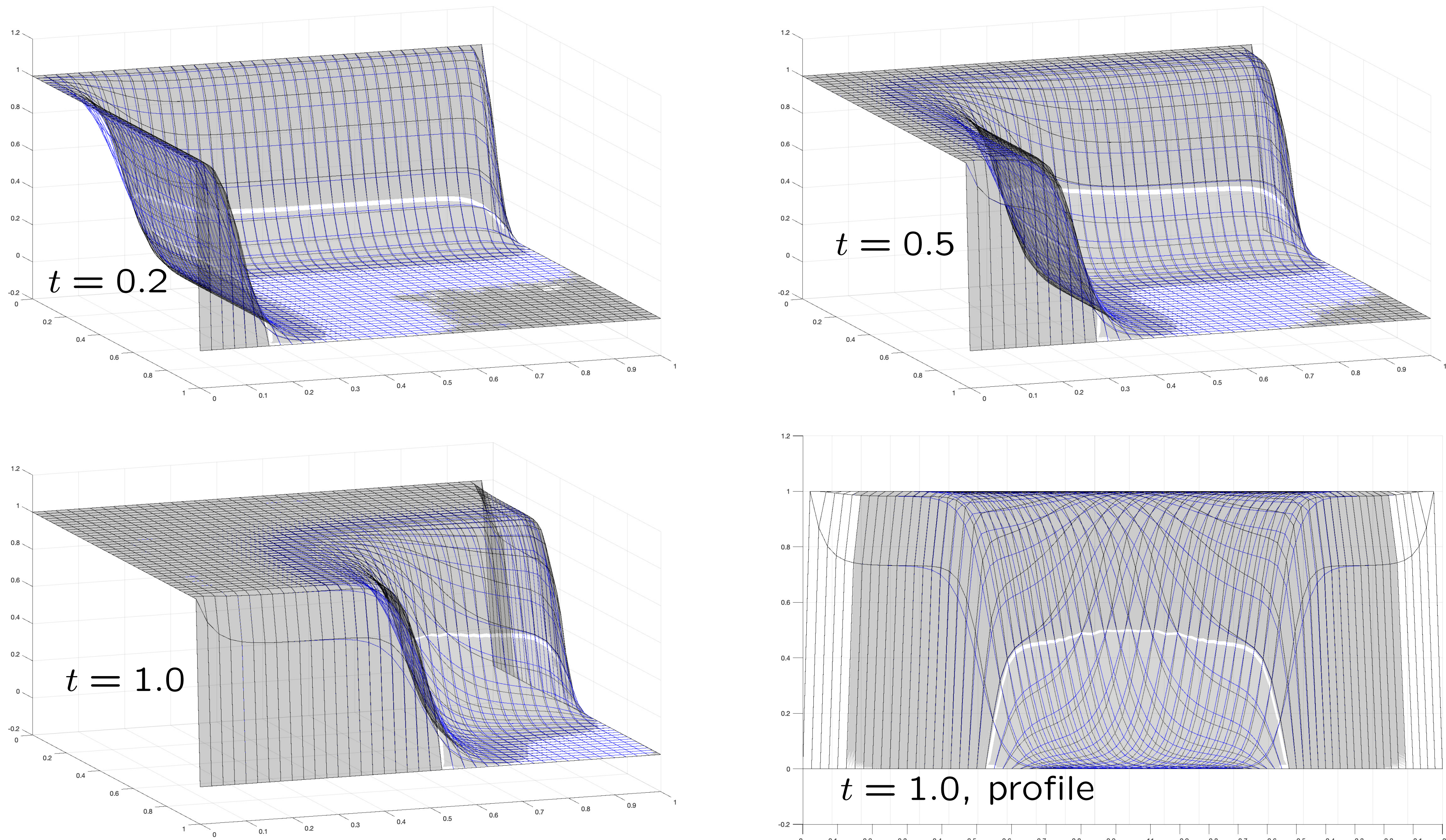

— backward Euler, CFL/2 — SATh-LF scheme $\bar{u}$

Buckley-Leverett Equation in 2D

$$u_t + \left(\frac{u^2}{u^2+(1-u)^2}\right)_x + \left(\frac{u^2}{u^2+(1-u)^2}\right)_y = 0 \quad \text{for } 0 < x, y < 1$$

$$\Delta x = \Delta y = 1/40,\ \Delta t = 1/10\ (\mathrm{CFL} = 8),\ \alpha_{\mathrm{LF}} = 2$$

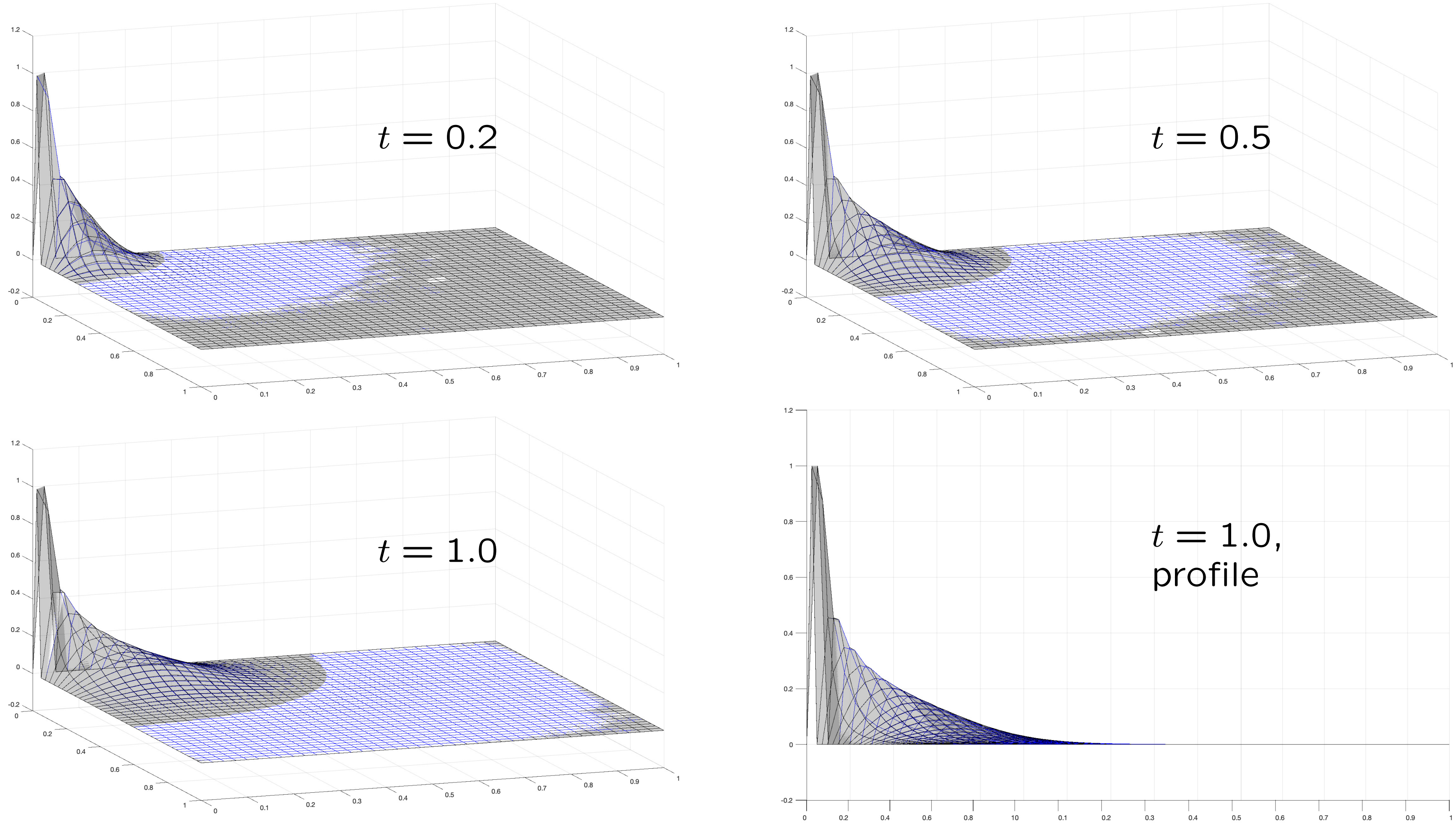

— backward Euler, CFL/2 — SATh-LF scheme $\bar{u}$

7. Summary and Conclusions

Summary and Conclusions — 1

$$\boxed{u_t + \nabla \cdot [f(u) - D(u)\nabla u] = 0}$$

Finite volume framework

- Space: use (implicit) WENO-AO reconstructions
- Time: use an adaptive, L-stable implicit, Runge-Kutta method

1. Locally conservative and captures the physics (advection, diffusion)
2. Only a few unknowns per mesh element per component (in n-D)

WENO-AO spatial reconstruction

1. High order accuracy when u is smooth, low order when discontinuous
2. Captures steep fronts ("essentially" non oscillatory)
3. Easy to extend to general 2D and 3D meshes

Adaptive Runge-Kutta time stepping

1. L-stable implicit Runge-Kutta (SSP not suitable)
2. $\Delta t \sim \Delta x$, chosen for accuracy, not stability
3. Adapt between Radau IIA and composite backward Euler
4. Radau accuracy when u is smooth, BE when discontinuous

Self Adaptive Theta scheme. A "better backward Euler"

1. The differential equation controls both $\bar{u}_i^{n+1}$ and $\bar{\bar{u}}_i^{n+1}$
2. These are used to define Discontinuity Aware Quadrature (DAQ)
   - Accurate locally to $\mathcal{O}(\Delta t^2)$, even with discontinuities
3. DAQ gives SATh schemes for conservation laws

$$\theta_i = \max\left(\frac{1}{2}, \frac{\bar{\bar{u}}_i^{n+1} - \bar{u}_i^n}{\bar{u}_i^{n+1} - \bar{u}_i^n}\right)$$

   The upstream scheme:

   - is stable for monotone fluxes
   - satisfies maximum principle for monotone flows and is TVB/TVD
4. Early stage of development:
   - less diffusive than backward Euler
   - the general SATh-LF seems to have all the good properties of BE
   - shows promise!

References

1. T. Arbogast and Ch.-S. Huang, *A Self-Adaptive Theta Scheme using Discontinuity Aware Quadrature for Solving Conservation Laws*, in preparation.
2. T. Arbogast, Ch.-S. Huang, X. Zhao, and D. N. King, *A third order, implicit, finite volume, adaptive Ringe-Kutta WENO scheme for advection-diffusion equations*, Comput. Methods Appl. Mech. Engrg. (2020), to appear.
3. T. Arbogast, Ch.-S. Huang, and Xikai Zhao, *Finite volume WENO schemes for nonlinear parabolic problems with degenerate diffusion on non-uniform meshes*, J. Comput. Phys. 399 (2019, to appear), DOI 10.1016/j.jcp.2019.108921.
4. T. Arbogast, Ch.-S. Huang, and Xikai Zhao, *Accuracy of WENO and Adaptive Order WENO Reconstructions for Solving Conservation Laws*, SIAM J. Numer. Anal. **56:3** (2018), pp. 1818–1847, DOI 10.1137/17M1154758.